Diversity of microbial metal sulfide biomineralization

Yeseul Park, Damien Faivre

Diversity of Microbial Metal Sulfide Biomineralization

Yeseul Park and Dr. Damien Faivre
Aix-Marseille Université, CEA, CNRS, BIAM, 13108 Saint-Paul-lez-Durance
yeseul.park@cea.fr; damien.faivre@cea.fr

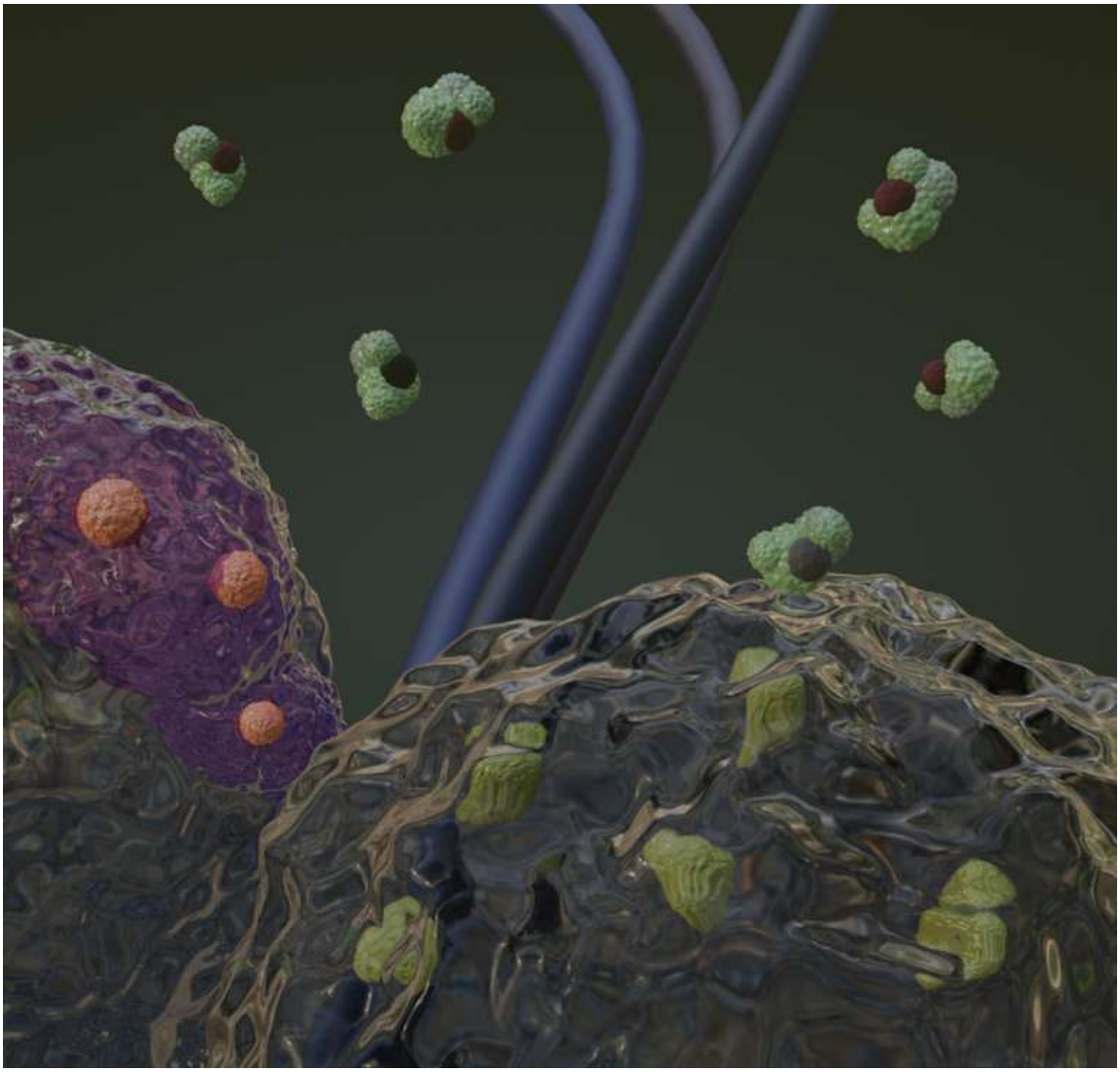

Abstract

Since the emergence of life on Earth, microorganisms have contributed to biogeochemical cycles. Sulfate-reducing bacteria are an example of widespread microorganisms that participate in the metal and sulfur cycles by biomineralization of biogenic metal sulfides. In this work, we review the microbial biomineralization of metal sulfide particles and summarize distinctive features from exemplary cases. We highlight that metal sulfide biomineralization is highly metal- and organism-specific. The properties of metal sulfide biominerals depend on the degree of cellular control and on environmental factors, such as pH, temperature, and concentration of metals. Moreover, biogenic macromolecules, including peptides and proteins, help cells control their extracellular and intracellular environments that regulate biomineralization. Accordingly, metal sulfide biominerals exhibit unique features when compared to abiotic minerals or biominerals produced by dead cell debris.

1. Introduction

Metals are essential for most biochemical reactions and more generally for life-related activities in microorganisms.[1] Key processes in the biogeochemical cycle of metal elements are associated with mineral immobilization and mobilization driven by microorganisms.[2] Immobilization of metal species involving biological processes is achieved through biomineralization, biosorption, and bioaccumulation.[3] Biomineralization is a metal precipitation process, in which inorganic particles are formed by organisms. In turn, biosorption refers to a metabolically-passive process where metals are bound to a cellular surface by simple adsorption. Finally, bioaccumulation involves energy-consuming processes where active transport systems are often required.[4] The biosorption and bioaccumulation frequently occur ahead of biomineralization processes.

In contrast, biological mobilization of metal species occurs through reactions involving redox potential changes, such as bioleaching and bioweathering. Mobilization of metal species commonly results in an increase of bioavailability of metals.[2] Bioleaching or biooxidation is a set of reactions in which minerals are oxidized by organic acids and organic compounds typically secreted by acidophiles.[5] Bioweathering is biological dissolution of minerals through mechanical and chemical reactions.[6] These reactions can occur via different mechanisms, depending on the metal sulfide types and associated microorganisms.[7]

Metal sulfide is one of the major family of minerals. It is ubiquitously encountered in global biogeochemical metal cycles.[8,9] In general, metal sulfide nanoparticles are common metal reservoirs and carriers in anoxic environments at low temperature.[10,11] Natural metal sulfides generally have a wide variation in chemical compositions, valence states, and crystal phases.[9] Metal sulfides are commonly divided into several categories depending on the structural features of the formed crystals, but most of the sulfide crystals in nature are subordinate to simple binary or ternary systems and contain impurities.[8] Metal sulfide nanoparticles have interesting and useful properties and functions,[13,14] in particular high electric conductivity and thermal stability.[15,16] Metal sulfides are typically diamagnetic, paramagnetic or Pauli-paramagnetic but several transition-metal sulfides such as greigite (Fe_3S_4) and pyrrhotite (Fe_7S_8) have a magnetic ordering leading to permanent magnetic moments.[17–19] Such magnetic property is used by organisms like magnetotactic bacteria that use intracellular magnetic nanoparticles composed of greigite, in order to migrate to the optimal conditions for their growth and proliferation by interacting with Earth's magnetic field lines.[20,21]

Precipitation and dissolution of metal sulfide frequently occur by the above-mentioned microbial

reactions. For example, precipitation of metal sulfides is reported both in the extracellular and in the intracellular space of sulfate-reducing organisms that produce reductive sulfur species. Metal sulfide biominerals are also often produced by other species of bacteria, archaea, and fungi as we will see below. The formation of metal sulfide nanoparticles is often correlated to metal detoxification, which is a process used by microorganisms to decrease the concentration of metals from their environment to reduce their toxicity.[22,23] Biomineralization that occurs promoted by high concentrations of metal ions as a microbial reaction to protect microorganisms from their toxicity is recently termed 'forced biomineralization' by H.Ehrlich et al. Hence, metal sulfide biomineralization becomes a good example of this biomineralization category.[24] On the contrary, metal sulfides can be dissociated by sulfide-oxidizing microorganisms in marine environments.[25][26,27] The dissolution of metal sulfides is mostly performed by biogenic oxidants at the exopolysaccharide (EPS) layer of microorganisms[28] after the cells attach on the mineral surface.[29] Bioleaching of metal sulfides has been widely studied for its significance and advantages in industrial purposes in the biomining industry.[30,31] Metal sulfide precipitation and dissolution also takes place by macroorganisms. For example, deep-sea gastropod mulluscs biomineralize iron sulfides with organic substrates to make their outer shell composed of pyrite or greigite. Bioleaching of pyrite is observed at plant roots of that secrete oxidant compounds.[32]

Similar to their role in the metal cycle, biogenic metal sulfides play an important role in the global sulfur cycle.[33–36] A critical process in the sulfur cycle is sulfate reduction, which involves dissimilatory sulfate reduction to sulfide, sulfur disproportionation, and sulfide oxidation.[35] The main driving force for sulfide generation in sediments is sulfate-reducing activities of microorganisms.[33,37] Many heavy metals can be sequestered by interactions among metal ions and biogenic molecules produced by sulfate reducing prokaryotes (SRP). For example, Co, Ni, Cu, Zn, Cd, As, Hg, and Pb are reported to effectively precipitate with sulfide anions.[38,39]

So far, there have only been a few reviews that concentrated on metal sulfide biominerals.[37,40,41] Therefore, we focus here on the extensive diversity of microbial metal sulfide biomineralization, and on important factors for each biomineral property, structuring the review based on the materials' composition. In general, metal sulfide biominerals show characteristic features that are distinguishable from abiotic precipitates. The types of metal sulfide biominerals are highly metal- and organism-specific. We remarked that many organisms produce and use proteins or peptides as capping agents for metal sulfide biomineralization. Capping agents are stabilizers of the surface of nanoparticles and regulate their growth or agglomeration.[42,43] Capping agents generally reduce the size of nanoparticles, thus work against Ostwald ripening that consumes smaller particles to grow particles into a larger size driven by surface energy. Throughout this review, we highlight the diversity in types and mechanisms of biomineralization. We anticipate that a comprehensive understanding of distinctive features from metal sulfide biomineralization will facilitate a systematic approach for understanding new types of biogenic metal sulfides and potentially other types of biominerals.

2. Classifications of biomineralization

Biomineralization can be grouped into several categories based on different criteria. The most commonly used criteria are (1) types of minerals based on chemical composition and crystal form of minerals,[44] (2) the degree of biological control,[45] and (3) the location of mineralization.[46] Metal sulfide biomineralization shows a wide variety in the degree of biological control involved and in the location of mineralization. In section 3, we organized different types of metal sulfide biominerals based on the criteria (1) and examined each biomineralization case further based on the criteria (2) and (3). Below is a summarized description of the last two criteria.

Based on the degree of biological control, biomineralization can be mainly categorized into three following groups. First of all, biologically-influenced biomineralization (BFM, Figure 1A) is a passive mineralization process occurring on cellular organic templates such as the bacterial cell wall and extracellular polymeric substance (EPS).[47,48] The main composition of EPS is polysaccharides, which also comprises of other types of polymers, such as enzymatic proteins, lipids, and extracellular DNA.[49] The composition and structure of EPS varies according to the microorganisms, accordingly the function as well.[50,51] The function of EPS varies but is mainly responsible for protection of microbial cells. Dependent on metal species, the contribution of polysaccharides or proteins for binding of metal ions to EPS could be different.[52] Cellular surface substrates commonly have a negative charge in both cases of gram-positive and gram-negative bacteria.[28,53] Positively-charged metal ions are easily stabilized when they are bound to the surface and locally supersaturated by electrostatic interactions.[54,55] Macromolecular crowding effect also affects macromolecular stability, effectiveness in functions based on alteration in protein folding and also mineralization behaviors both in promotion and inhibition of nucleation.[56] With the assist of organic substrates on the surface of bacteria, nucleation and crystallization of amorphous minerals is several orders of magnitude faster than what it is for pure inorganic mineralization.[55] Even dead or disrupted debris from cells are sufficient to function as a substrate that promotes supersaturation and further nucleation and growth of minerals.[57]

Second, biologically-induced biomineralization (BIM, Figure 1B) is defined as the precipitation of inorganic materials in the environment driven by cellular activities. This class of biomineralization involves active reactions between metabolic byproducts and environmental solutes that lead to nucleation and maturation of minerals in the environment.[55] It has been proposed in the literature that the end products formed by this type of biomineralization are not distinguishable from precipitates produced by purely inorganic reactions and that the reaction typically occurs outside the cell but in the close vicinity of the cell surface.[55]

The last category, biologically-controlled biomineralization (BCM, Figure 1C), refers to the precipitation of minerals by elaborate cellular control inside a separated compartment. The most important feature found in this class of biomineralization is the association with an organic matrix that forms an isolate intracellular environment, thus the group was formerly referred as organic matrix-mediated biomineralization.[58,59] The cellular compartment, such as a vacuole or an organelle like the magnetosome, maintains a different condition from that recorded outside to facilitate supersaturation of minerals. This is possible due to the guidance of proteins and macromolecules embedded in the surrounding matrix. The biological control is applied in several processes: transport of the necessary chemical elements to the nucleation site and direction of the precipitation to particular structures or phases. To be more specific, the organisms control the crystal habit, the crystal organization, the localization of nucleation, the chemical composition, and the crystal phase.[60] However, only a few reported cases found in microorganisms satisfy all the criteria for this biomineralization category. Despite of the involvement of a biogenic organic matrix, many biomineralization cases show less control over some material properties of the biomineral, such as calcium carbonate inclusions found in cyanobacteria that shows amorphous crystal structures and no specific chemical composition.

Biomineralization can also be classified based on the location of mineralization. All reported cases are broadly categorized into four groups as follows: extracellular, epicellular, intracellular, and intercellular.[46,61] These terms refer to biomineralization occurring outside the cell, on the surface of cell, inside the cell, and in between cells, respectively.

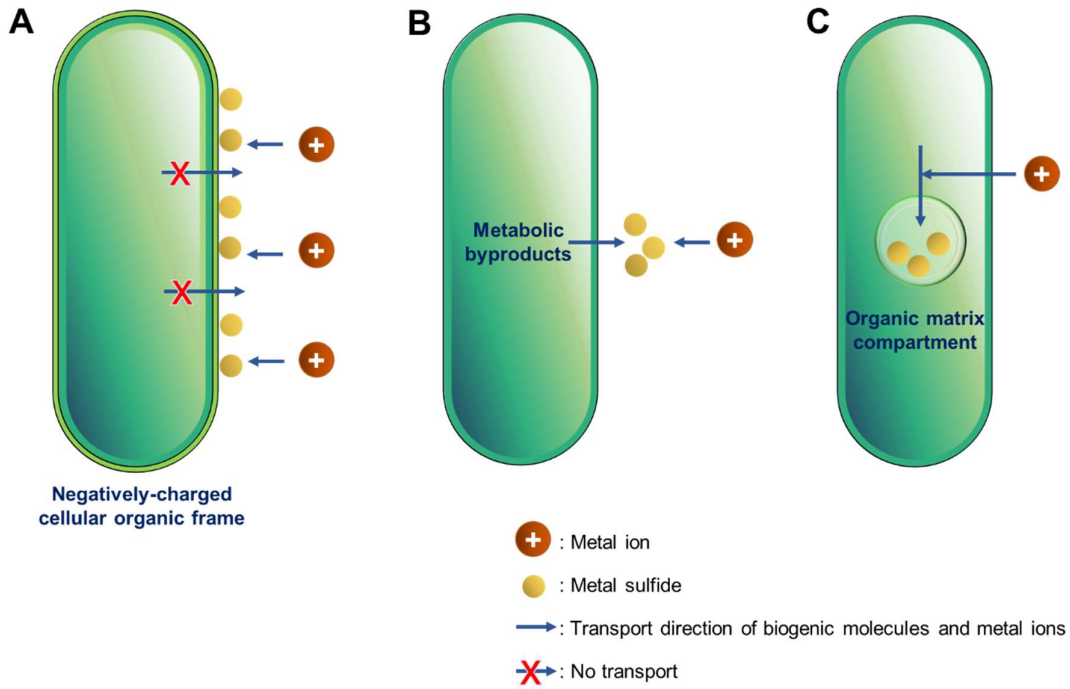

Figure 1. Schematic illustration of three major types of microbial biomineralization that are conventionally categorized by the degree of biological control. (A) Biologically-influenced biomineralization (BFM) that primarily takes place through passive reactions between the cellular substrate and metal ions from environments. (B) Biologically-induced biomineralization (BIM) that occurs by metabolic byproducts reacting with environments. (C) Biologically-controlled biomineralization (BCM) that involves cellular compartments for the precipitation of biominerals in a controlled way that cannot be achieved by abiotic reactions.

3. Features of metal sulfide biomineralization cases

3.1. Iron sulfides

Iron sulfides are the most common metal sulfide species. They are typically found in anoxic sediments.[62–64] Iron sulfide minerals can be produced by pure chemical reactions and include greigite (Fe_3S_4), pyrrhotite (Fe_7S_8), mackinawite (tetragonal FeS), pyrite (cubic FeS_2), marcasite (orthorhombic FeS_2), and amorphous FeS.[55,65] Compared to these abiotic iron sulfides, those formed by SRB and anaerobic archaea are limited to amorphous FeS, mackinawite, greigite and rarely pyrite.[37,66,67]

Microbial cultures have the ability to crystallize iron sulfide minerals much faster than what it is observed in abiotic conditions. For example, SRB culture produces crystalline mackinawite in a week, whereas abiotic experiments require several months.[68] Rapid production of sedimentary pyrite is attributed to sulfate reduction by microorganisms as well, although pyritization is not common in bacterial culture and still requires several weeks at least.[68,69] The kinetics of phase transformation from mackinawite to gregite is also influenced by microorganisms that accelerate the formation of gregite.[70] As such, microorganisms play a significant role in the dynamics of iron sulfide mineralization.

Iron sulfide biominerals appear in various morphologies, especially when they are associated with cellular substrates. A few iron sulfide biomineralization cases were reported to encrust the cellular

substrates with different morphologies, with the biomineralization being dependent on the composition of the cellular templates and the types of bacteria.[37,70–72] Intracellular biomineralization of presumptive amorphous iron sulfide particles has been observed in SRB *Desulfotomaculum nigrificans* and *Desulfovibrio desulfuricans*, but not observed in the *Escherichia coli* at the same high iron concentrations.[73] Most of the intracellular particles appear to precipitate within the periplasmic area and such a process shows features of both BIM and BCM.[55]

The highest control in microbial metal sulfide biomineral formation is observed in greigite magnetosome nanoparticles produced by magnetotactic bacteria (MTB).[37,38] MTB form intracellular magnetic nanoparticles composed of either magnetite (Fe_3O_4) or greigite (Fe_3S_4) to align themselves along the Earth's magnetic field lines.[74] MTB are single cells (Figure 2) or multicellular aggregates named multicellular magnetotactic prokaryotes (MMP) (Figure 3). Greigite producing MTBs are sulfate-reducers,[75] which belong to the *Deltaproteobacteria* phylum.[75] The material properties of the iron sulfide particles are controlled by magnetosome proteins that are typically located in a specific zone of a gene cluster called the magnetosome island.[76][77] The proteins are either mostly embedded in the membrane of an organelle called magnetosome or work together with the organelle to nucleate, maturate, and organize greigite magnetosome particles.[40]

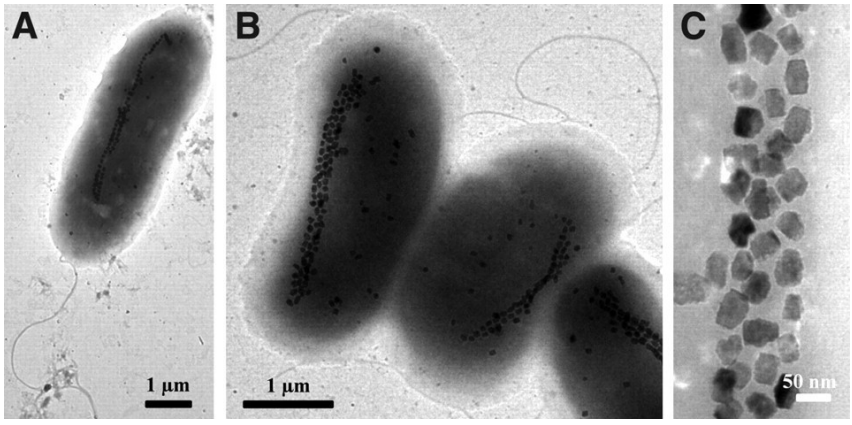

Figure 2. TEM images of uncultured magnetotactic bacteria (MTB) and greigite- and/or magnetite magnetosomes. (A and B) MTB cells collected from a spring in the Great Boiling Springs geothermal field in Gerlach, Nevada, USA. (C) High-magnification image of greigite crystals from the cell shown in (B). (Figure adapted from [78] with permission)

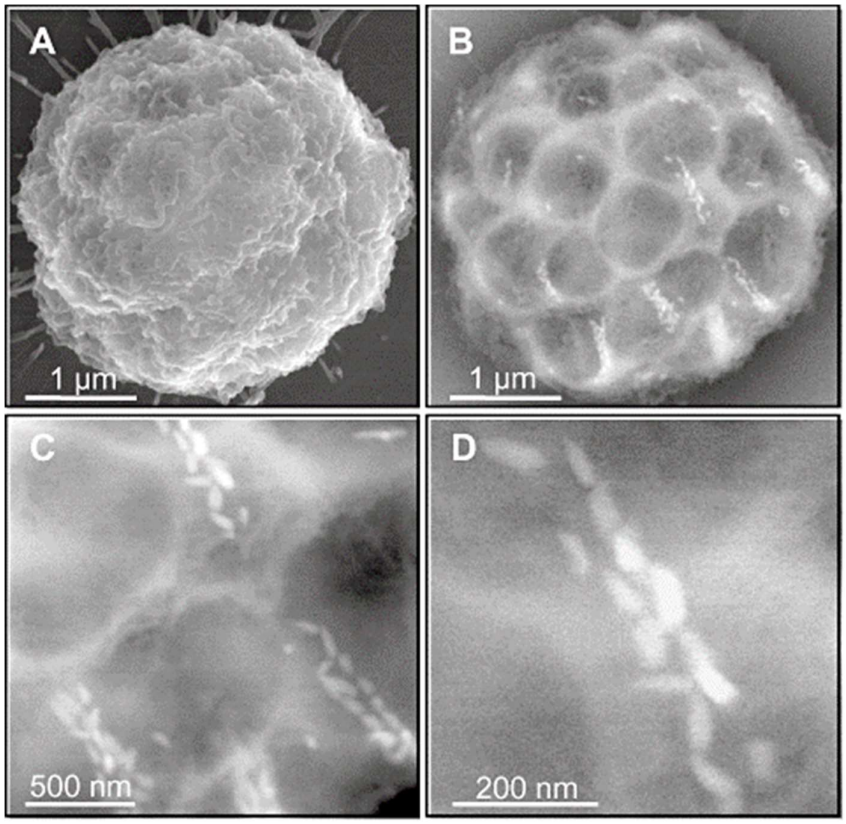

Figure 3. SEM images of an uncultured multicellular magnetotactic prokaryote (MMP) and greigite magnetosomes. (A) Secondary electron image showing filamentous surface structures in a MMP. (B) Back-scattered electron image that reveals the arrangement of single cells within the individual MMP. The rows of magnetosomes can be distinguished based on their high yield of back-scattered electrons, which results in a bright signal. (C) Greigite magnetosomes are arranged in a few parallel chains. (D) Magnified image on two greigite magnetosome chains in (C). All magnetosome crystals are bullet-shaped, 91 ± 21 nm long and 40 ± 6 nm wide, and show a similar orientation. (Figure adapted from [79] with permission)

Greigite magnetosome particles show strict biological control over nearly all possible particle properties, including particular mineralization location, crystal dimension, chemical composition, as well as crystal organization. Magnetosome iron sulfide particles fall within the size of single domain state (less than 120 nm).[80] The ideal crystal habits of magnetosomes include cubo-octahedrons, truncated octahedrons, or rectangular prisms (Figure 4).[81,82] Bullet-shaped or arrow-head greigite particles have also been reported in greigite magnetosomes (Figure 3).[66,79] Finally, irregular shapes have also been observed.[67]

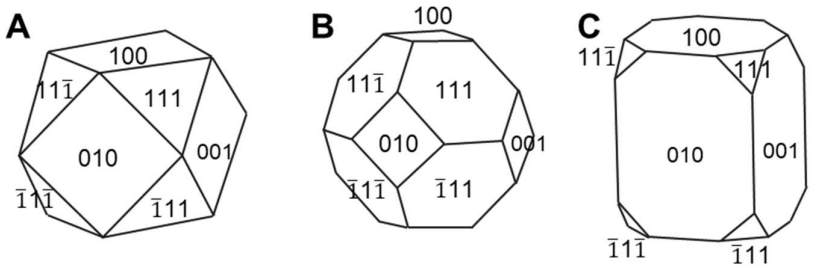

Figure 4. Crystal habits suggested as ideal greigite crystals found in magnetotactic bacteria. (A) Cubo-octahedron. (B) Truncated octahedron. (C) Truncated rectangular prism.

Historically, pyrrhotite ($Fe_{1-x}S$) and pyrite (FeS_2) were proposed as possible phases of greigite magnetosome particles possibly originating from a misinterpretation of the electron diffraction data of the crystal structure.[83,84] Indeed, M. Posfai et al. later examined several environmental samples and suggested that the diffraction data rather indicated greigite, mackinawite and cubic FeS of the sphalerite structure.[85] They also observed crystal diffraction patterns of magnetosomes and found that a mackinawite particle inside a dead MTB cell transformed into greigite after several days of exposure to air, suggesting mackinawite as a precursor of greigite magnetosome particles. Accordingly, greigite is regarded as the final phase of greigite magnetosome nanocrystal after repeated phase transformation processes. The irregularity of the surfaces, stacking faults and lattice strains found on greigite particles also imply that they originate from the structural remnant of mackinawite during structural transformation.

As a summary, iron sulfide biomineralization occurs with varying degrees of biological control. Iron sulfide biomineralization can take place anywhere: on the cell wall, within biofilms, in the extracellular region, in the periplasmic space, and also in a cellular organelle in the cytoplasm (Table 1). Among the iron sulfide cases, the most striking case is the precipitation of greigite in magnetosomes, which represents one of the most highly controlled biomineralization pathways satisfying all of the aspects of biological control defined for BCM.[40] In contrast, extracellular biomineralization of iron sulfides on the cell surface shows random properties corresponding to a combination of BFM and BIM. Each case shows distinguishable characteristics in morphology, phases, and size from minerals produced via abiotic processes.

3.2. Mixed metal sulfides containing iron

In the environment, iron sulfide minerals typically contain different trace elements. One example is pyrite particles containing Ni, Cu, Zn, As, Mo, Ag, and Pb.[86,87] Iron sulfide precursors incorporate other metal by adsorption, chemical substitution and coprecipitation.[88] These additional elements can accelerate or inhibit the conversion to more stable structures, such as Fe-containing copper sulfides that transform into Fe-Cu-sulfides,[10] or iron sulfides reacting with arsenic by sorption that are inhibited to convert to pyrite.[89]

Dissolved iron in the microbial environments affect biomineralization of other metal sulfides and contrariwise. For example, the metal concentration needed for initial metal sulfide precipitation and the

properties of the biogenic materials are affected by the presence of other metal species: a high concentration of Ni in the *Desulfotomaculum* DF-1 culture hinders the formation of FeS since Fe-complexation is increased, while Ni remains soluble during the precipitation of FeS, because the bacterium also secrets Ni-binding proteins.[90] The amount of iron species that adhere to the cell surface decreases when the concentration of nickel increases in the medium. M. Mansor et al. particularly investigated the influence of the ratio between the concentration of Ni and Fe on biomineral properties of mixed metal sulfides composed of Ni and/or Fe.[91] Even trace amount of iron increases the time needed to develop crystallinity in nickel sulfide precipitates, which can cause better solubility of Ni to easily dissolve Ni back into the environment. On the contrary, Ni incorporation into mackinawite (FeS) enhances the stability of mackinawite. Figure 5 presents the influence of biological contribution on mineralization of mixed metal sulfides in conditions of different Ni / Fe concentrations. The phase, crystallinity, size and morphology differ according to the biological influence.

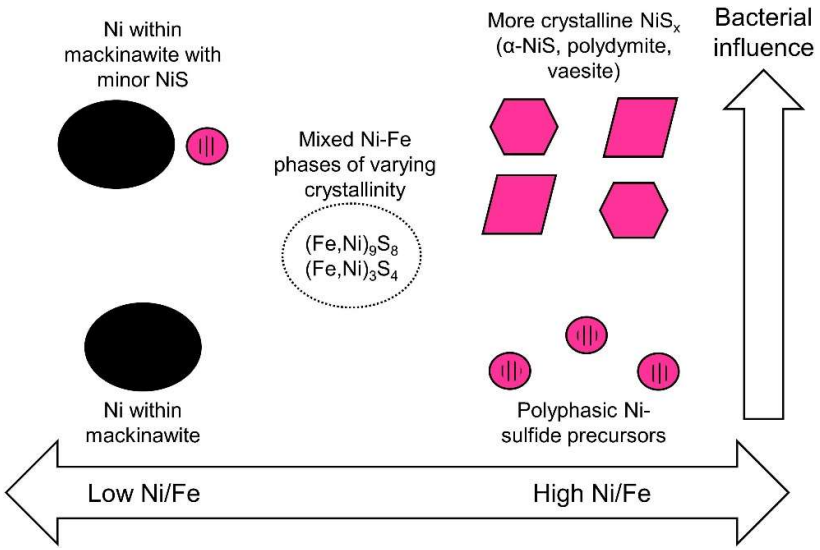

Figure 5. Schematic diagram of the predicted Fe and Ni-hosting phases in environments of low redox potential and high concentration of sulfur. The mineral properties are determined by the initial $[Ni]_{aq}/[Fe]_{aq}$ ratios in solution and by the degree of bacterial influence. Bacterial culture influences on iron sulfide with different metals (Reproduced with permission from [91])

Following the same line, but with Fe and Cu, SRB produce Fe-Cu sulfides, of which the crystallinity is enhanced by the presence of dissolved Fe.[37,92] It is an opposite tendency from nickel sulfide biominerals that shows less crystallinity in the presence of dissolved Fe. In comparison to abiotic systems, biogenic Fe-Cu sulfides show higher selectivity in particle composition, and crystal structure.[10] SRB cultures also accelerate the transformation of Fe-rich copper sulfide to become mixed metal sulfides by atomic rearrangements, from covellite into chalcopyrite or nukundamite.[10] Contrary to an earlier hypothesis that chalcopyrite is formed only by the reaction between iron sulfides and aqueous Cu,[93] the transformation from covellite to chalcopyrite occur through redox reactions between aqueous Fe and S atoms present in covellite with the supply of sulfur from bisulfide ions (HS^-).

Intracellular biomineralization of Fe-Cu sulfides have been reported in uncultured magnetotactic bacteria producing greigite magnetosome particles.[66,94] Significant amounts of copper inclusion in greigite magnetosomes often occur in the microorganisms, of which the degree is variable roughly

between 0.1 to 10 atomic percent of iron content in magnetosome particles.[66] M. Posfai et al. observed that mackinawite converted to greigite from the same crystals when there was no significant amount of Cu, while disordered mackinawite crystals containing Cu remained in the same crystal structure without phase transition.[66] Accordingly, it is speculated that the inclusion of copper affects the conversion rate from mackinawite to greigite to inhibit the phase transformation. Besides, Bazylinski et al. suggested that this copper inclusion could be related to heavy metal detoxification.[94]

Biomineralization of mixed metal sulfides is more complicated than the single metal version since the concentration of a metal influences the biomineralization of other metal sulfides. This directly influences the properties of the formed biominerals, in terms of crystallinity, size, morphology, crystal defects, and even phase. The variations originating from the inorganic factors seem based on BIM but the biological control by metal-binding proteins is highly involved as well. Compared to magnetite magnetosomes, greigite magnetosomes seem more affected by the influence of other metals, by copper, in particular.

3.3. Nickel sulfides

All the cases of nickel sulfide biomineralization presented on Table 1 are based on extracellular biomineralization achieved by metabolic activities of SRB. The structure of biominerals identified in these studies include vaesite (α-NiS), heazelwoodite (Ni_3S_2), polydymite (Ni_3S_4), millerite (trigonal NiS), or amorphous phase. In comparison with abiotic precipitates produced by sulfide sources, the biomineralized nickel sulfide precipitates showed more ordered crystallinity, different size, as well as different crystal phases (Table 1).[91,95,96] The solubility and crystallinity change in nickel sulfide phases is attributed to pH change and traces of other metals.[91] The presence of organic capping agents also influences the properties of nickel sulfide biominerals.[90,97] The solubility of nickel sulfide indeed increases in the microbial culture due to the organic capping agents that are secreted by bacteria. These factors, as well as the slower release of biogenic sulfides responsible for the decreased reaction speed of biomineralization, are recognized as the main contributors of the crystallinity of nickel sulfide biominerals.

Nickel sulfide biomineralization commonly shows characteristics of BIM, as the biominerals are mainly produced by reactions between metabolites and metal ions in the culture. However, SRB control the solubility of nickel ions in the culture by secreting biomolecules. Accordingly, they control the biomineralization processes, which in turn influences the biomineral properties as well.

3.4. Copper sulfides

Copper sulfide biomineralization is reported to efficiently remove dissolved copper from a microbial culture.[98] Extracellular copper sulfide biomineralization by SRB produces CuS (covellite) or Cu_2S (chalcocite). Biogenic nanoparticles have a tissue-like morphology showing smaller size, less crystallinity and less resistance to dissolution than abiotic counterparts.[92] This tendency is opposite to what has been observed in other types of biogenic metal sulfides that mostly show better crystallinity and resistance against dissolution.[91,99,100] Moreover, the tissue-like morphology may not be only attributed to the slow speed of the reaction between metabolic byproducts and the environment. Other biomolecules possibly work as a guiding substrate for the morphology. A particular case of extracellular biomineralization of copper sulfide is seen in the culture of the fungus *Fusarium oxysporum* where peptides are possibly helping produce spherical particles in the narrow size range of 2-5 nm.[101] This

implies that also in this case, potential capping agents are involved in the control of the morphological and chemical properties of biominerals, similarly to what is found in many other metal sulfide biominerals.

Intracellular biomineralization of copper sulfide, in turn, has been recently reported in the culture of the metal-reducing bacterium *Geobacter sulfurreducens*.[102] This microorganism is a sulfur-reducing organism, and does not have genes to exert dissimilatory sulfate reduction for metal sulfide production. Accordingly, this biomineralization points towards a unique mechanism for the sulfur resources used for this biomineral production. This is magnified by the fact that the bacterium also forms epicellular and extracellular biominerals on top of the intracellular ones.

The biological control of copper sulfide biomineralization, therefore, appears at different degrees. Each biomineralization case reflects a high biological influence, which possibly includes biomolecules that control the mineralization process. Although the involvement of an organic matrix in the biomineralization processes is unclear, the reported cases cannot be described simply based on BIM.

3.5. Zinc sulfides

Microbial zinc sulfide biomineralization has been widely reported, not only in SRB cultures but also in the culture of a purple bacterium, a thermophilic anaerobic bacterium, and different fungi (Table 1). In general, zinc sulfide biomineralization is influenced by the activities of biogenic organic molecules. In environmental samples collected from a peatland, zinc sulfide biominerals are associated with organic matters that become the carbon source for bacteria (Figure 6). The organic matter found in the samples is suggested to be a main player of the observed framboidal morphology in aggregates.[103]

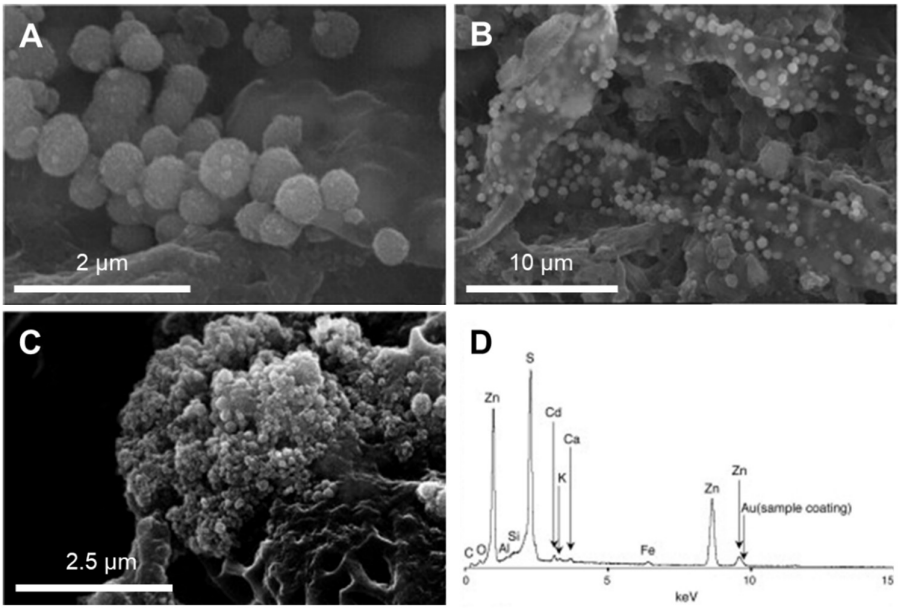

Figure 6. SEM images and EDX spectrum of ZnS framboidal aggregates discovered in anoxic peat samples from the Big Muck. (A) Typical morphology of zinc sulfide particles obtained from peats. (B) ZnS particles embedded in unidentified organic residues. (C) Particles found in humidified peat samples. (D) Energy-dispersive X-ray spectrum of one of ZnS framboidal aggregates in (C). (Figure adapted from [103] with permission)

A few zinc sulfide biomineralization cases associated with biofilms also present tightly regulated particle size (less than 5 nm) and defined crystal structures.[104,105] The bacterial biofilm involved in such highly-controlled biomineralization could be regarded as a frame that controls particle morphology, as well as an efficient means to transport the organic molecules, metal ions, and sulfide sources required to produce the nanoparticles. Microbial extracellular biomineralization within biofilms possibly functions in a similar way to what is observed in eukaryotic biomineralization where an extracellular frame is involved in the control of the biomineral properties, in particular the morphology.[106–108]

Extracellular zinc sulfide are produced by the anaerobic bacterium *Serratia nematodiphila*. They are composed of fine nanocrystals with an average size of 7 nm that become the building blocks of larger aggregates. The particles were suggested to bond with proteins through amide or aliphatic residues.[109] The yeast strain *Aspergillus flavus* also uses capping agents for extracellular biomineralization.[110] In this case, the zinc sulfide nanoparticles are coated with the capping agents via amine groups and cysteine residues.

In summary, zinc sulfide biominerals commonly show many features attributed to strict biological control based on the role played by capping agents or biomolecules embedded in EPS. This is remarkably not limited to the formation of intracellular particles, but also observed in the case of simple extracellular biominerals.[104] Accordingly, biomineralization is more than a simple reaction between metabolites and the environment, and microorganisms seem to exert biological control over many reactions related to biomineralization.

3.6. Arsenic sulfides

The phases discovered in arsenic sulfide biomineralization include AsS (realgar), As_2S_3 (amorphous, orpiment), As_4S (duranusite). The type of arsenic sulfide biominerals depends on the culture conditions, including pH and redox potential. For example, the pH value affects the cellular activities and metabolism, such as efficiency of sulfate reduction and arsenic reduction from As^V to As^{III} in the bacterial culture. A mixed culture of anaerobic bacteria showed 8 times higher efficiency in sulfate reduction at pH 7.1 than at pH 6.1.[111] The decrease in the sulfate reduction rate leads to more reduction of arsenic ions and the rate of formation between As^{III} and H_2S in turn influences the biomineral formation.

An example is found in the sulfate-reducing *Desulfotomaculum Auripigmentum*. Intracellular biomineralization of arsenic sulfide was observed as the encrust in the cell and appeared together with epicellular and extracellular biomineralization.[112] The intracellular precipitation seems associated with a cytoplasmic membrane and located within the periplasmic space. However, the particles generally do not show a specific control in their morphology or distribution within the cell. This biomineralization is not solely biologically-induced but involves cellular control on a few points such as the particle composition and crystal phase. Epicellular precipitates confined within a membrane-like compartment show a potential involvement of EPS for biological control over biomineralization at the cell surface.

Another interesting case is arsenic sulfide precipitates with the morphology of filamentous nanotubes that were observed in the culture of the metal-reducing bacterium *Shewanella* sp. HN-41 (Figure 7). The biomineral has a diameter ranging between 20 and 100 nm and the average length of 30 μm. A phase change occurs in this biomineral with time: amorphous As_2S_3 is first formed and then transformed to realgar and to duranusite.[113,114] Exopolysaccharides-based substrates are associated with the production of the filaments. The EPS is suggested to serve as the substrate, thereby explaining the

morphology.[113,115] The nanotubes show metallic conductivity after several days of aging because of deposition of elemental As on them and also photoconductivity at the exposure of UV. Other *Shewanella* strains also produce arsenic sulfide-based filamentous nanotubes but show similar radial structure functions from the EXAFS spectra of *Shewanella* sp. HN-41, thereby indicating slight differences in mineral compositions, in turn supposedly related to different reduction rates.[114] Similar multiphase biomineralization is often discovered in biominerals produced by eukaryotes, such as a diatom *Didymosphenia geminata*, which produces a nanofibrous framework based on multiphase calcium carbonates using a polysaccharide matrix.[116]

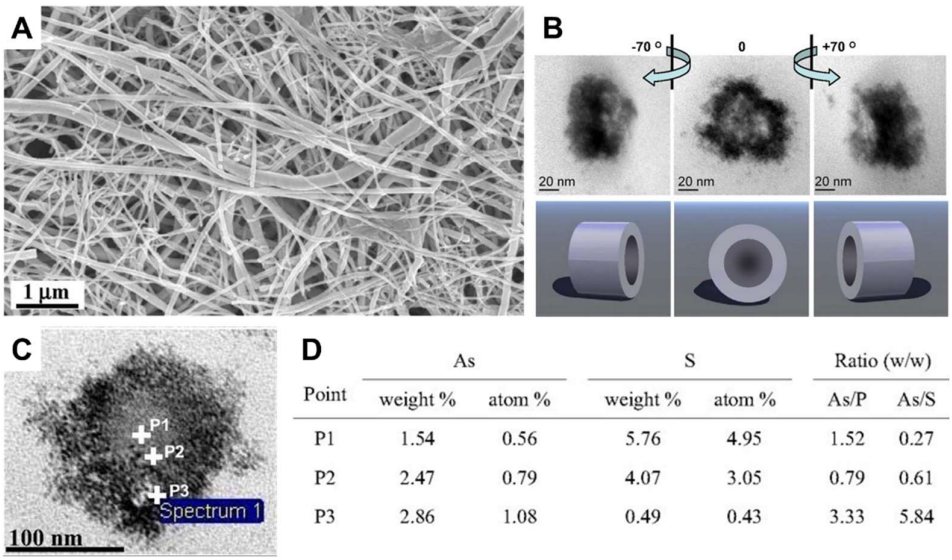

D

Point	As		S		Ratio (w/w)	
	weight %	atom %	weight %	atom %	As/P	As/S
P1	1.54	0.56	5.76	4.95	1.52	0.27
P2	2.47	0.79	4.07	3.05	0.79	0.61
P3	2.86	1.08	0.49	0.43	3.33	5.84

Figure 7. Electron micrographs and chemical analysis of biogenic As-S nanotubes. (A) SEM image. (B) Cross-sectioned TEM tomograms. (C and D) STEM-EDX point spectra from the cross-section of one of the As-S nanotubes. (Figure adapted from [113] with permission, Copyright (2007) National Academy of Sciences, U.S.A.)

A final notable case observed in the environment is the mineralization on cell substrates by hot flow enriched with hydrogen sulfide that goes through open cracks of fungal colonies.[117] This process forms a specific morphology following the former arrangement of cells. The precipitation of filamentous clusters shows a similar composition to orpiment at the hydrothermal sites.[117] This type of biomineralization has not been defined by conventional classification for biomineralization types but could be close to BFM as the dead cell frame composed of organic materials affects the morphology of biominerals.

In summary, and as in most cases depicted so far, the biomineralization of arsenic sulfides cannot be simply classified with features distinctive of BFM, BIM, and BCM. In the example of arsenic sulfide nanotubes produced by *Shewanella* species, the cellular surface and EPS are involved in the biomineralization as in BFM. The EPS, however, can offer a compartment for controlling the particular morphology, in a similar way to what is observed in BCM. The biomineralization is also influenced by metabolic byproducts and environmental factors, as in BIM.

3.7. Cadmium sulfides

Crystal phases of cadmium sulfide biominerals that have been reported to include rock-salt, zinc-blende, wurtzite, and amorphous phases (Table 1). In order to produce cadmium sulfide, sulfate reduction and cysteine degradation are used as the main pathways to utilize sulfur sources, while cadmium ions are supplied in excess to the culture. For example, supplementing the culture of the deep-sea bacterium *Idiomarina* sp. OT37-5b with cysteine results in cysteine degradation, thereby producing H_2S in the bacteria, and in turn CdS production on the cell surface.[118] CdS biomineralization on the surface of cells could also promote energy production as well as reduce the Cd stress. It implies that cadmium sulfide biominerals potentially perform other functions than the protection from heavy metal stress in the environment.

In order to produce CdS nanoparticles, some microorganisms use proteins that not only reduce sulfate or cysteine but also work as capping agents. For example, a putative cystathionine γ-lyase (smCSE) produced by the aerobic gram-negative bacillus *Stenotrophomonas maltophilia* strain SMCD1 mediates a reaction between cadmium acetate and L-cysteine to direct the synthesis of nanocrystals of 2 to 4 nm (Figure 8).[119] As a control, bulk CdS precipitates without size regulation when the enzyme is absent. Similarly, a deep-sea bacterium *Pseudomonas stutzeri* 273 uses an enzyme called threonine dehydratase (psTD) that can control the size and structure, as well as to produce H_2S from L-cysteine.[120] This enzymatic activity ends up producing wurtzite precipitates composed of nanocrystallites of about 4 nm in size. A fungus *Fusarium oxysporum* can also secret sulfate reductases into the environment in order to produce stable extracellular cadmium sulfide particles in the size range between 5 and 20 nm.[121]

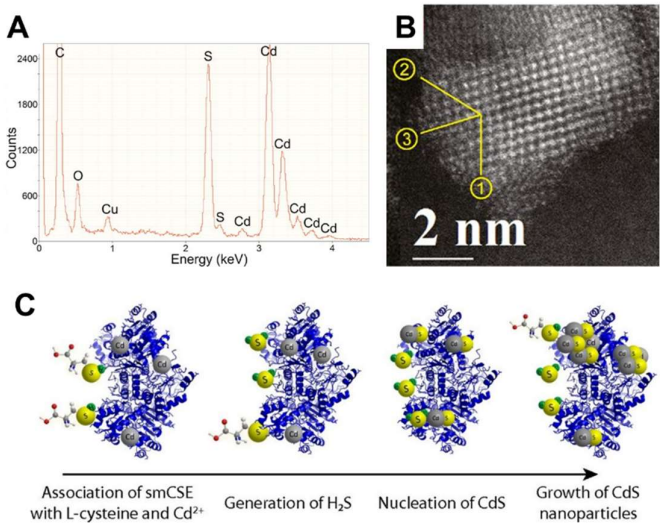

Figure 8. Features of extracellular cadmium sulfide biominerals produced by the single enzyme smCSE and the schematic biomineralization process. (A) XEDS spectrum confirming the coexistence of Cd and S in the nanocrystals. (B) A HRTEM image of wurtzite CdS nanocrystal viewed along [211] projections. (C) Schematic of proposed CdS quantum dot synthesis by smCSE. smCSE associates with cadmium acetate and L-cysteine present in solution, smCSE degrades L-cysteine to produce H_2S, H_2S produced by smCSE nucleates CdS nanoparticles, and CdS nanoparticles continue to grow upon the continuous generation of H_2S. (Figure adapted from [119] with permission)

Yeasts also use peptide-based capping agents, such as phytochelatins (PC_n), to precipitate cadmium sulfides, both inside and outside the cells.[122] Phytochelatins have been found in plants, fungi, algae and cyanobacteria and is typically produced by the catalytic activity of an enzyme called PC

synthase.[123] The length of the peptide is determined by the concentration of heavy metals. The production of peptides is especially activated by cadmium, compared to other heavy metals.[124] The complex PC-Cd(II) can also further integrate sulfide ions to form intracellular cadmium sulfide nanoparticles and be stored in cytoplasmic vacuoles by the activity of HMT1 (Figure 9D).[125,126] *Saccharomyces cerevisiae* and *Schizosaccharomyces pombe* showed similar diameters in their PC-CdS complexes (about 2 nm), but different crystal diffraction patterns.[122] Figure 9 shows the distribution of cadmium and sulfur elements, as well as cadmium sulfide biominerals within vacuoles of two yeast species *S. pombe* and *Candida glabrata*.[127] The process of biomineralization occurs within the cytoplasm and vacuoles of the yeast. This biomineralization process involving the activity of capping agents to control the biomineralization was classified as a type of matrix-mediated biomineralization.[128]

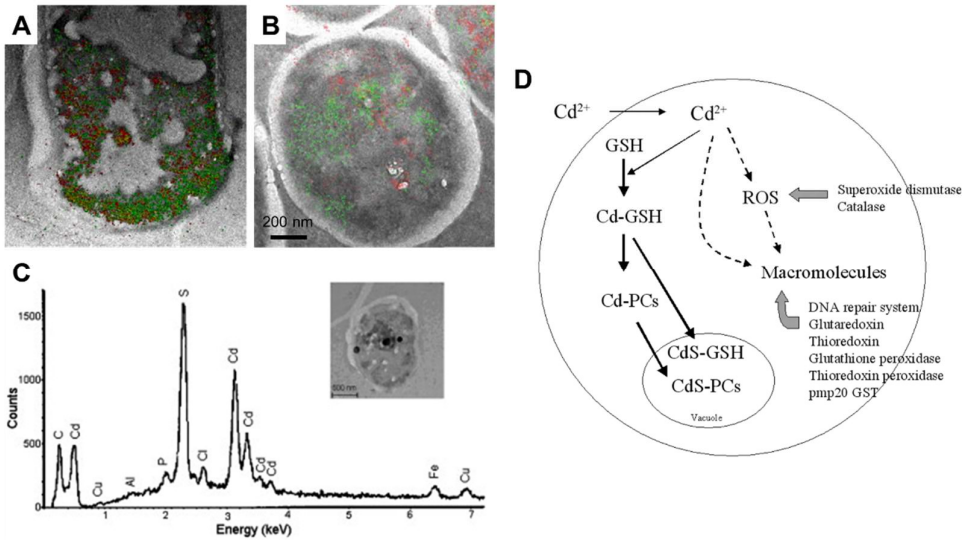

Figure 9. Features of intracellular (cytoplasmic) cadmium sulfide biominerals produced by yeast species and the schematic biomineralization process. (A, B) EFTEM-ESI images of *S. pombe* (A) and *C. glabrata* (B) (Cd : red, S : green). (C) EDX spectrum of the element composition of a selected area in a *C. glabrata* cell presented in the inset. (D) A model for the cadmium (Cd^{2+}) detoxification in *S. pombe*. Free cellular Cd^{2+} ions are scavenged initially by GSH, later by PCs, and eventually sequestered into the vacuoles as a form of nanocrystalline CdS capped with either GSH or PCs. Cd^{2+} ions escaped from the complexation damage from the cellular macromolecules either directly or via the production of ROS. The cells overexpress superoxide dismutases and catalase to remove the ROS and other detoxification proteins to restore the damaged macromolecules. (Figure adapted from [126] and [127] with permission)

As such, biomineralization of cadmium sulfide depends on several mechanisms and appears in various microorganisms. As presented in Table 1, the size of nanocrystals of cadmium sulfide generally shows a narrow size distribution and dimensions below 20 nm, regardless of the localization of precipitation. For the control over particle properties, one single protein or a set of proteins can be associated or involved in the compartmentalization of the particles. The particle properties cannot be obtained by simple inorganic reactions with metabolites and metal ions in the environments. Rather, microorganisms need to produce adequate biomolecules to capture certain metal ions, and further treat them to react with reductive sulfur species. The nanoscopic capping agents composed of cellular organic matrix lead to the regulation of particle properties by creating conditions to supersaturate nanoparticles within the nanoscopic compartment. As mentioned also in other metal sulfide cases, the production of the capping agents can be regarded as an active cellular control over metal ions in their environments, and the type

and size of capping agents also depend on the environmental conditions. Especially for cadmium sulfide, the capping agent complex is further transported into a cellular organelle, which facilitates the biomineral sequestration and storage. Although biominerals created in such a manner lack particular crystal habits and organization, the cellular activities for this biomineralization and associated biological control are relatively closer to BCM than BIM.

3.8. Lead sulfides

Lead sulfide biominerals are typically associated with a cubic PbS structure and small particle size. The bacterium *Lysinibacillus sphaericus* SH72 produces extracellular particles of 4 to 10 nm in size.[129] In this case, L-cysteine is not only used as a sulfur source by the bacteria but also as a stabilizing agent of PbS nanocrystals. According to the S-H vibration bond and the EDX spectrum, the presence of organic molecules surrounding particles was proposed.[129]

Yeast species, such as *S. pombe* or *Torulopsis*, are also known to biomineralize CdS but intracellularly.[130] The particle size ranges from 2 to 5 nm. Capping agents composed of biopolymers are associated with the biomineralization. Intracellular biominerals with similar size distributions are also reported in the marine metal-tolerant yeast *Rhodosporidium diobovatum* (Figure 10).[131] PbS biomineralization is a widespread phenomenon that also occurs within the periplasmic space in other *Candida* species, but as opposed to CdS or HgS biomineralization, it does not appear within vacuoles in the cytoplasm.[132] Intracellular biomineralization of lead sulfide has been also reported in a marine bacterium *Idiomarina* sp. strain PR58-8 that synthesizes quantum dots consisting of tetragonal PbS_2 with a particle size varying between 2 and 10 nm.[133]

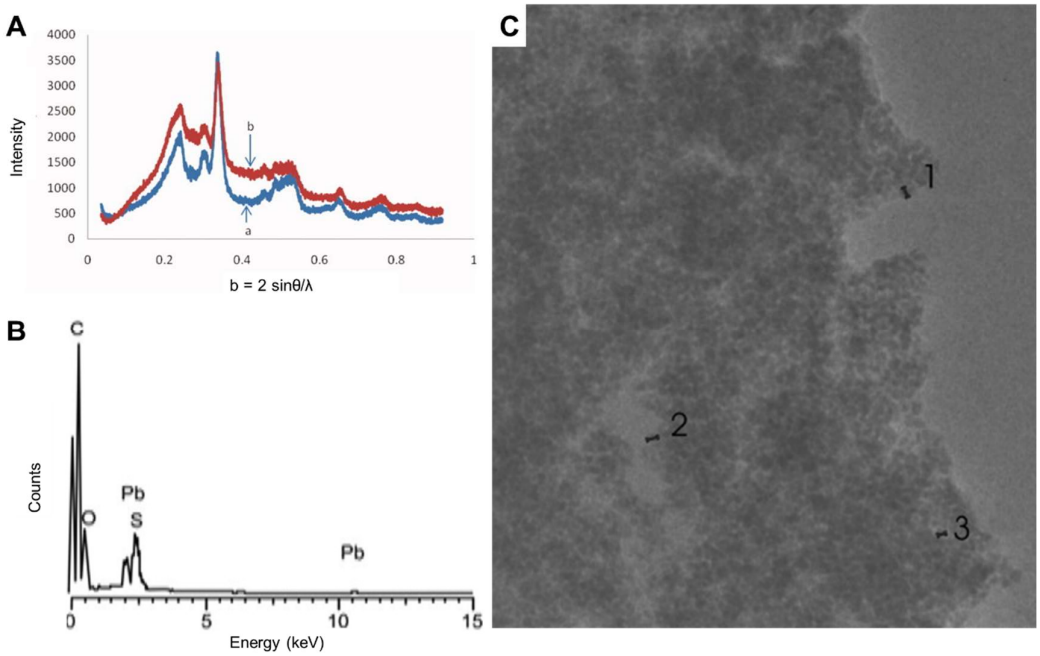

Figure 10. Features of intracellular (periplasmic) lead sulfide biominerals produced by *R. diobovatum*. (A) XRD of PbS nanocrystallites (a) at 96 h and (b) after 6 months of storage. (B) EDX analysis of lyophilized cell pellets containing PbS nanoparticles. (C) TEM micrographs of lyophilized cell pellets containing the PbS nanoparticles. Sizes of bars 1: 6.16 nm, 2: 6.68

nm, and 3: 4.81 nm. (Figure adapted from [131] with permission)

Both extracellular and periplasmic lead sulfides commonly show regulation in the size of the biomineral, and in their crystal phase. The lead biomineralization cases occur with active cellular production of biomolecules so that the cells can treat lead ions in their intracellular and extracellular environments. Especially periplasmic biomineralization cases include a surrounding organic matrix composed of chelating molecules along with possible restraints within the periplasmic space. Despite displaying less biological control compared to cytoplasmic biomineralization, the biomineralization of lead sulfides shows some factors matching that of BCM.

3.9. Other metal sulfides

Biomineralization of metal sulfides includes silver sulfide. Silver sulfide nanoparticles composed of Ag_2S are produced using bacteria species such as *Pseudomonas stutzeri* AG259, which deposit Ag_0 and Ag_2S particles sized of up to 200 nm in the periplasmic space (Figure 11).[134] In the mixed bacterial culture of *Thiobacillus ferroxidans* and *Thiobacillus thiooxidans*, acanthite (Ag_2S) granules are produced on the surface of the bacteria in the presence of sulfide anions and silver cations.[135] Finally, the yeasts *Candida albricans* and *Candida glabrata* also biomineralize extracellular Ag_2S compounds.[136]

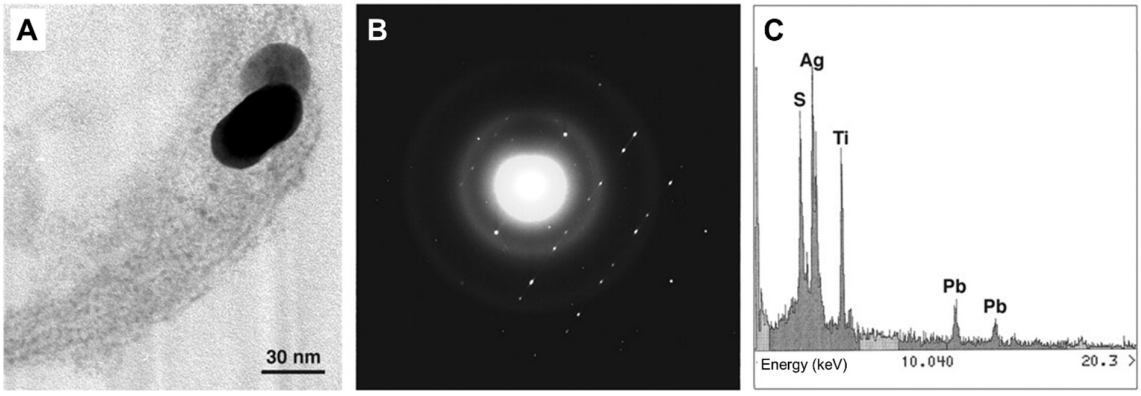

Figure 11. Features of intracellular silver sulfide biominerals produced by *P. stutzeri* AG259. (A) A silver sulfide particle embedded in the periplasmic space of the cell. (B) Crystal diffraction pattern analysis on one of the particles. (C) EDX spectrum and electron diffraction indicating monoclinic Ag_2S. (Figure adapted from [134] with permission, Copyright (1999) National Academy of Sciences, U.S.A.)

A final example is the biomineralization of mercury sulfide in the yeasts *Candida glabrata*, *Candida krusei* and *C. parapsilosis.* These biomineralize extracellular and intracellular mercury sulfide microparticles in acidic conditions.[132] The intracellular biominerals appear to be stored in a vacuole as in cadmium sulfide biomineralization. As opposed to cadmium sulfide nanoparticles, which are distributed over the cell with controlled size to remain as nanoparticles, mercury sulfide particles mostly stay agglomerated in a few regions within the cell.

4. Summary and outlook

Here, we have reviewed the microbial metal sulfide biomineralization providing a comprehensive overview of the known biomineral diversity. A large variety of biomineralization mechanisms were identified, depending on both the metal species and the microorganism. The breadth of metal sulfide microbial biomineralization is summarized in Table 1 and schematically presented in Figure 12. Briefly, metabolic byproducts obtained from bioreduction of sulfur-containing molecules are first released and then react with metal ions to produce the biominerals. This process can be mediated by a single or multiple biogenic macromolecules. For example, biopolymers from EPS, which cover the cell surface, contribute to biomineralization and thereby further control the properties of biomineralized particles, such as their size, composition and morphology. Proteins and peptides produced by microorganisms are released into their intracellular space as well as the extracellular environments to regulate the metal toxicity by chelating the dissolved metal ion species. A peptide like phytochelatin can chelate heavy metal ions, sequester metal sulfide particles in and out of the cell, and further store the particles within a cytoplasmic organelle.

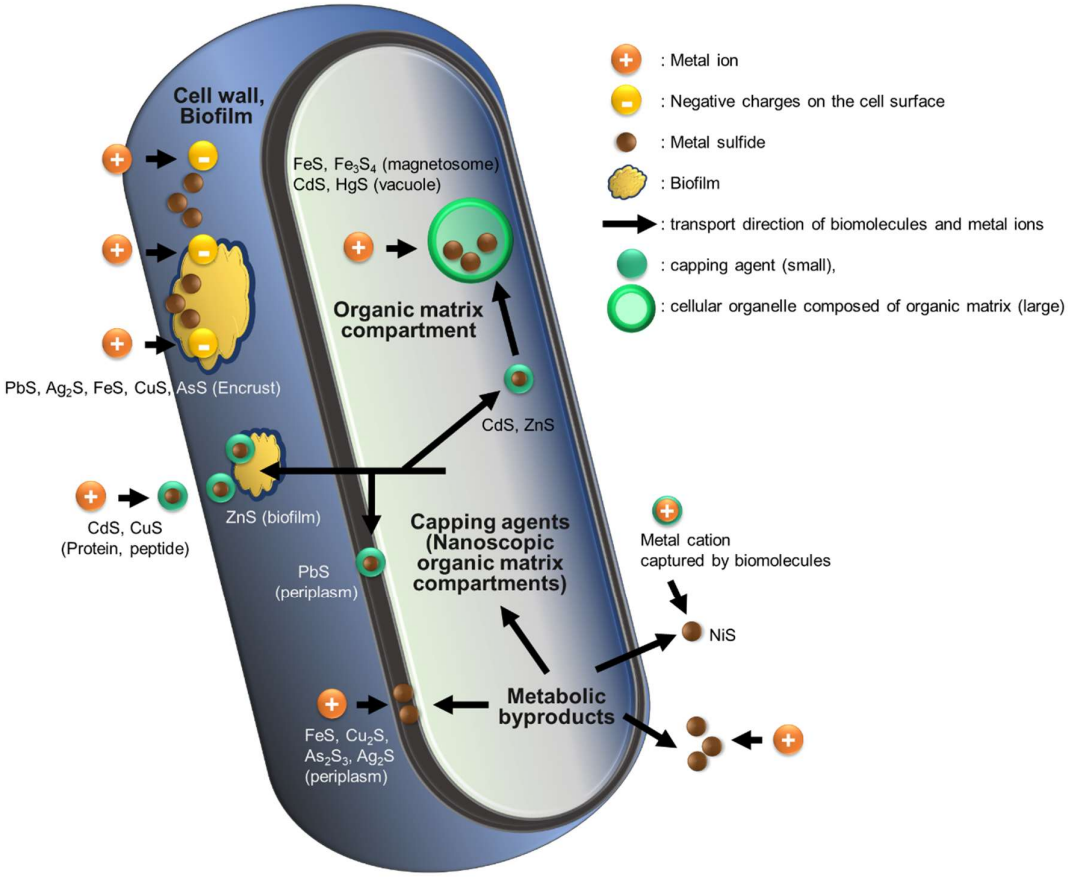

Figure 12. Schematic illustration on types of metal sulfide biomineralization processes in an alive microorganism. Metal ions react with metabolic byproducts as well as other types of biogenic organic molecules, such as capping agents or components from cell substrate or biofilms. Depending on metal species, microorganisms use different strategies of biomineralization for protection and other life activities.

For the biomineralization process, microorganisms use various mechanisms to control different metal species in the environment or in the cell as their resources. Microbial cells import or decrease concentration of metal ions by releasing biomolecules in the environment, export metal ions back into the extracellular environments, or even store them in different cellular locations. For sulfur resources, the H_2S production through sulfate reduction or L-cysteine degradation is the main driving force of the process.

Extracellular metal sulfide biomineralization results in that the biominerals have distinguishable chemical and/or morphological features from abiotically-produced precipitates obtained under the same condition. E. Peltier *et al.* suggested that the properties of these biogenic metal sulfide particles originate from a slower release rate of H_2S into the environment than what typically occurs with abiotic syntheses.[39] Molecular crowding effect and surface charges from the cells could also contribute to general properties of biominerals. Moreover, the properties of many extracellular metal sulfides biominerals are controlled by organic matrices, such as peptides, proteins or biofilm components, which exert a control over the particle composition, crystal structure, shape, size, resistance to dissolution, and/or agglomeration of nanocrystallites.

In contrast, the highest control in metal sulfide biominerals is found in the intracellular formation of iron sulfide magnetosome particles, which satisfies all the criteria for BCM. Cadmium sulfide and mercury sulfide biomineralization have also been observed in cellular organelles, within cytoplasmic vacuoles, while some cadmium sulfide particles appear to stay captured in capping agents within the cell. Some intracellular biomineralization cases, such as in iron sulfide cases, were reported in the periplasmic space as well. The latter generally show features obtained in the biologically-induced or less controlled manner, which results in random size distribution or morphology of the particles. Compared to those cases, periplasmic lead sulfide biomineralization shows a higher control over size distribution, composition or morphology, originating from the involvement of biomolecules working as capping agents.

4.1. Remark on the classification of biomineralization based on the degree of control

Following environmental changes, microorganisms actively control gene transcription, biomolecule production, and sometimes type and speed of their metabolism. Even slight changes in environmental factors can accordingly lead to distinct particle properties in biomineralization processes. Therefore, the reactions of microorganisms to environmental factors can be regarded as a type of cellular control that microorganisms exert over biomineralization as well. Such biological controls, however, are not adequately presented by the conventional description of BIM. In addition, both BFM and BIM mostly occur together in living organisms, especially in the epicellular biomineralization cases. Therefore, the distinction between BFM and BIM is not clear apart from the BFM case occurring by dead cell debris.

The distinction between BIM and BCM is intricate and ambiguous as well. Indeed, nanoscopic capping agents, composed of proteins or peptides, could be regarded as a compartment to generate isolated environments for precipitation of metal sulfides. The polymeric capping agents, that are often found in extracellular biomineralization, lead to unique features in material properties. C. T. Dameron and D. R. Winge previously described the biomineralization involving peptides as organic matrix-mediated biomineralization,[58,128] which is a former term for BCM.[137] Other example is EPS-based arsenic sulfide nanotubes that show morphological controls with variable chemical compositions. Such cases

589 show all the aspects of BFM, BIM and BCM. In addition, R. B. Frankel and D. Bazylinski already
590 mentioned that many intracellular cases, such as vacuolar inclusions, which correspond to the cadmium
591 sulfide or mercury sulfide biominerals, are difficult to be classified under one category either BIM or
592 BCM.[55]

593 Therefore, and as A. Veis suggested, it might not be useful anymore to clearly distinguish among
594 conventional categories of biomineralization based on the degree of control in biomineralization.[60]
595 Rather it is important to understand the degree and range of the biological control for each type of
596 biomineralization, which could help in the understanding of the biomineralization mechanisms.

597

598 **Table 1. Types and features of metal sulfide biominerals and factors influencing their biomineralization**

Metal sulfide	Phase	Organism	Morphology (Size, shape)	Factor for biomineralization or other information	Location	Comparison with abiotic precipitates or pure BFM	Ref
Iron sulfide	FeS_2 (pyrite), FeS (mackinawite)	Desulfovibrio desulfuricans	Flake-like aggregates, thin biofilm of FeS, hundreds of nm Spherules within the film	The presence of ferric phosphate nanoparticles (for pyrite formation)	Extracellular, Biofilm	Different morphology (framboidal pyrite in the abiotic condition)	[68]
	Fe_3S_4 (greigite), FeS (mackinawite), FeS_2 (pyrite)	Mixed culture of SRB consortium (Lake Pavin, France)	Rounded beads, spherules, encrust	Aging (the size of spherules and phases)	Extracellular, epicellular	Different phase (Pyrite and greigite only detected in the biological condition)	[69]
	Fe_3S_4 (greigite), FeS (mackinawite), FeS2 (pyrite)	Thermococcales	Cuboidal, irregular, 30-70 nm	Biofilm, extracellular vesicle	Extracellular (biofilm)		[138]
	Fe_3S_4 (greigite), FeS (mackinawite)	Desulfovibrio hydrothermalis AM13	Irregular, tissue-like, Encrust	Incubation time (for greigite formation)	Extracellular, epicellular	Larger aggregates than abiotic condition but smaller than dead cell debris, more growth than nucleation of mackinawite, greigite only in the biotic condition	[69]
	Fe-S (amorphous)	Desulfotomaculum nigrificans, Desulfovibrio desulfuricans	Irregular, 10-50 nm	Bacteria type (Not observed in Escherichia coli, apart from when sulfide is treated)	Intracellular, extracellular	Different morphology (more separated than when sulfide is provided)	[73]
	$Fe_{1-x}S$ (pyrrhotite), FeS_2 (marcasite), FeS (mackinawite)	Desulfovibrio vulgaris	Encrust in periplasm, Spherical, oval, 20-200 nm	Electron uptake and metabolic rate are faster with precipitates	Intracellular, extracellular, epicellular		[139]
	FeS (mackinawite-like)	Desulfotomaculum sp. DF-1	Encrust, hundreds of nm random aggregates		Extracellular, epicellular		[90]
	FeS (amorphous, mackinawite), Fe_3S_4 (greigite)	Desulfovibrio vulgaris	4.4 nm (pH 8.6, 4 days), 12.6 nm to 23.9 nm (pH 6.9, 16 days)	pH value, sulfide accumulation (accelerating transformation)	Extracellular		[140]
	Fe_3S_4 (greigite)	Desulfamplus Magnetovallimortis strain BW-1	Pleomorphic, lacking well-defined crystal habit	Magnetosome proteins	Intracellular		[78]
	Fe_3S_4 (greigite)	Uncultured MTB (Single cell MTB, Morro Bay, CA, USA)	~ 60 nm, Width/length ratio 0.2-0.4 in elongated particles, axis of elongation parallel to the magnetosome chain, Fe oxide shell	Magnetosome membrane and proteins	Intracellular		[20]
	Fe_3S_4 (greigite), FeS (mackinawite), Cubic FeS (tentative presence)	Uncultured MTB (single cell MTB and MMP, Morro Bay, CA, USA)	Equidimensional or slightly elongated, 30-120 nm	Magnetosome membrane	Intracellular		[66]
	Fe_3S_4 (greigite)	Uncultured Candidatus Magnetomorum litorale (MMP, Wadden Sea, Germany)	Bullet-shaped, a few arrowhead-shaped, 91 ± 21 nm (length) and 40 ± 6 nm (width)	Magnetosome proteins	Intracellular		[79]
	Fe_3S_4 (greigite)	Uncultured Candidatus Magnetoglobus multicellularis (Araruama Lagoon, Brazil)	Pleomorphic, average 88 nm (length), 71 nm (width)	Magnetosome membrane and proteins	Intracellular		[141]
	Fe_3S_4 (greigite)	Uncultured MTB (MMP, Lake Yuehu, China)	Rectangular, 102 ± 14 nm (length) and 78 ± 13 nm (width)	Magnetosome membrane and proteins	Intracellular		[142]
	Fe_3S_4 (greigite), FeS_2 (pyrite - later disputed)	Uncultured MTB (MMP, Salt Pond, MA, USA)	Roughly cuboidal, parallelepipedal, flake-shaped, irregular, average 75 nm		Intracellular		[143]
Mixed metal sulfide containing iron	NiS, Fe/NiS, FeS	Desulfotomaculum sp. DF-1	Encrust, random aggregates	Ni-binding polypeptides, Bacterial surface	Extracellular, epicellular	Ni inhibits FeS production	[90]
	Polyphasic (millerite, polydmite, violarite, mackinawite, pentlandite dependent on Ni/Fe ratio)	Desulfovibrio vulgaris DSM 644	Spheroidal, 100-200 nm	Aging (better crystallinity), pH value (more Fe ratio in the particle), Fe concentration (smaller particle, less crystallinity)	Extracellular	Different phase, more crystallinity, larger size, crystal structure distortion by substitution	[91]
	Fe-rich covellite, nukundamite ($Cu_{5.5}FeS_{6.5}$), chalcopyrite ($CuFeS_2$), Cu-rich mackinawite	Desulfovibrio vulgaris DSM 644	Nanocrystals, nanorods, nanoplates, a few large aggregates (100-200 nm) of fine crystals	Cu/Fe ratio (larger particle in higher Fe concentration), pH value, Chalcopyrite is formed through incorportation of Fe into covellite	Extracellular	Similar morphology, larger size, lower crystallinity	[10]
	Cu-containing magnetosome of Fe_3S_4 (greigite), FeS_2 (pyrite - later disputed)	Uncultured MMPs (Morro Bay, CA, USA)	Pleomorphic	Cu/Fe ratio differs in particles from the same organism (0.1 to 10 at%)	Intracellular		[94]
	Cu-containing magnetosome of Fe_3S_4 (greigite), FeS (mackinawite), Cubic FeS (tentative presence)	Uncultured MMPs and single cell MTBs (Different places)	Equidimensional or slightly elongated, 30-120 nm	Cu content (slower transformation)	Intracellular		[66]
Nickel sulfide	Ni-S, Co-S	Mixed culture of SRB		Ni-binding protein, concentration of other metal	Extracellular	Higher solubility of Ni	[144]
	α-NiS, NiS (amorphous)	Mixed culture of Desulfosporosinus auripigmenti and Citrobacter freundii	Aggregates and encrust of fine particles (< 5 nm)		Extracellular, epicellular	Better crystallinity (amorphous in the abiotic condition)	[95]
	Ni_3S_2 (heazelwoodite), NiS2 (vaesite at 60℃)	Mixed culture of SRB	Disordered, tissue-like	Incubation time (thinner morphology), higher temperature (better crystallinity)	Extracellular	Different phases (mix of heazelwoodite and vaesite in the abiotic condition), Better crystallinity	[96]
	α-NiS, NiS_2 (vaesite), Ni_3S_4 (polydymite)	Desulfovibrio vulgaris DSM 644	Spheroidal vaesite (< 20 nm), euhedral (100-300 nm), irregular polydymite (10-20 nm)	Presence of other metal	Extracellular	More crystallinity, different morphology	[91]
Copper sulfide	CuS (covellite)	Desulfovibrio vulgaris DSM 644	Nanocrystals (<10 nm), nanorods (20-40 x 6-9 nm), nanoplates (~30 nm)		Extracellular	Smaller size, less crystalline	[10]
	CuS (covellite)	Mixed culture of SRB	Tissue-like	Higher temperautre (better crysallinity)	Extracellular	Different morphology, smaller size, less resistance, less crystallinity (related to slower precipitation rate)	[92]
	Cubic Cu_2S	Fusarium oxysporum	Spherical, 2-5 nm, surrounded by spherical peptide shells (20 nm)	Potential peptide (20 nm shell)	Extracellular		[101]
	CuS, Cu_2S	Mixed culture of SRB		Extracellular polysaccharide (enhancing Cu concentration)	Extracellular (biofilm)		[145]

	Cu_2S (chalcocite)	Geobacter sulfurreducens	Spherical, 10-90 nm	Anoxic condition	Intracellular, extracellular, epicellular	Smaller size (100-200 nm in BFM by dead cell debris)	[102]
Zinc sulfide	ZnS (similar to sphalerite, amorphous)	Desulfovibrio sulfuricans		Production speed	Extracellular	More crystalline, more resistance to oxidation	[39]
	ZnS (wurtzite, sphalerite)	Uncultured SRB (peatland near Manning, NY, USA)	Framboidal aggregates, 12-14 nm (wurtzite), ~ 48 nm (sphalerite)	Seasonal change (organism types), other metal impurity (stacking fault), organic matter debris (morphology)	Extracellular		[103]
	Cubic ZnS	Rhodobacter sphaeroides	4 nm (25 h), 12 nm (35 h)	Culture time	Extracellular (Intracellular nucleation and discharged)		[146]
	ZnS (sphalerite)	Uncultured SRB of the family Desulfobacteriaceae (Piquette Pb-Zn mine, WI, USA)	Spherical aggregates (< 10 μm) of fine particles (2-5 nm)	Biofilm	Extracellular (biofilm)		[147]
	ZnS (mainly sphalerite, wurtzite)	Uncultured SRB (Piquette mine, WI, USA)	Spheroidal aggregates (1-5 μm) of fine particles (1-5 nm)	Polymeric coating	Extracellular (biofilm)		[105]
	Hexagonal zinc sulfide	Aspergillus flavus	Spherical, 18-60 nm (DLS), 12-24 nm (TEM) (due to the presence of ionic layer)	Capping agent (protein)	Extracellular, epicellular		[110]
	Cubic ZnS	Serratia nematodiphila	Spherical aggregates (80 nm) of fine spherical particles (average size 7 nm)	Nucleation effect, presence of proteins binding with the particles	Extracellular		[109]
	ZnS (sphalerite)	Thermoanaerobacter	Aggregates (21.5 ± 6.0 nm, 11.8 ± 2.7 nm) of fine particles (2-10 nm, depending on thiosulfate concentrations)	pH value, aging, concentration of salts (sulfur source)	Extracellular		[148]
	Cubic ZnS	Saccharomyces cerevisiae MTCC 2918	30-40 nm		Intracellular, extracellular		[149]
Arsenic sulfide	AsS, As_2S_3	Mixed culture of As^V-reducing and SO_4^{2-} reducing bacteria	Aggregates of fine particles, encrust	pH value	Extracellular, epicellular		[111]
	As_4S_4 (β-realgar)	Clostridiaceae strain YeAs	Encrust, dendritic, tissue-like	Anaerobic condition	Extracellular, epicellular		[150]
	As_2S_3 (orpiment)	Uncultured fungal colonies from seafloor (several locations)	Filamentous nanotube	Hot flow enriched with H_2S	Entire cells of fungal colony killed by hydrothermal fluid	Different phase and morphology	[117]
	As_2S_3 (amorphous), realgar (AsS), duranusite (As_4S)	Shewanella sp. HN-41	Filamentous nanotube, 20-100 nm (diameter), ~ 30 μm (length)		Extracellular		[113]
	As_4S_5, AsS, and As_4S_3	Shewanella sp. strain HN-41, S. alga BrY, S.oneidensis MR-1, S. putrefaciens CN-32	Filamentous nanotube, 10-100 nm (diameter, depending on species)		Extracellular		[114]
	As_2S_3	Desulfotomaculum auripigmentum	Irregular, encrust		Intracellular, extracellular, epicellular	Less sensitive to sulfide or pH value	[112]
Cadmium sulfide	CdS	Pseudoalteromonas sp. MT33b	Cuboidal	Promoted by cysteine	Epicellular		[151]
	CdS	Idiomarina sp. OT37-5b	Cuboidal, irregular	Promoted by cysteine, Potential association of particles with harvesting energy through light energy	Epicellular		[118]
	CdS (amorphous)	Clostridium thermoaceticum	Starved cells : amorphous with small electron-dense granules	Promoted by cysteine	Extracellular, epicellular		[152]
	CdS (wurtzite)	Escherichia coli	2-5 nm	Capping agent	Intracellular, extracellular		[153]
	CdS (six-coordinate rock-salt structure)	Schizosaccharormyces pombe	Aggregates of fine particles (1.8 nm)	Capping agent (phytochelatin)	Intracellular, extracellular		[128]
	CdS (intermediate between rock-salt and the naturally occurring zinc-blende four-coordinate structure)	Candida glabrata	Aggregates of fine particles (2 ± 0.3 nm)	Capping agent (phytochelatin)	Intracellular, extracellular		[128]
	CdS (Zinc-blende structure)	Stenotrophomonas maltophilia strain SMCD1	2-4 nm	Capping agent (smCSE)	Extracellular		[119]
	CdS (wurtzite)	Pseudomonas stutzeri 273	84.53 nm, crystallite size of 3.7 ± 0.4 nm	Capping agent (psTD also as a catalytic enzyme, L-cysteine also as a substrate)	Epicellular		[120]
	Hexagonal CdS	Fusarium oxysporum	5-20 nm	Secretion of sulfate reducing enzymes	Extracellular		[121]
	Cubic CdS	Rhodopseudomonas palustris	8.01 ± 0.25 nm	Intracellular enzymes	Extracellular (Intracellular nucleation and discharged)		[154]
	Cubic CdS	Rhodobacter sphaeroides	Spherical, 2.3 ± 0.15 (36 h), 6.8 ± 0.22 (42 h), and 36.8 ± 0.25 nm (48 h)	Culture time, C-S-lyase	Intracellular, extracellular		[146]
Lead sulfide	PbS (galena)	Bacillus cereus sp. Abq	4-10 nm	Anaerobic condition, Promoted by cysteine	Extracelllar, epicellular	Different phase (no PbS formation in abiotic condition)	[155]
	Cubic PbS	Lysinibacillus sphaericus SH72	Spheroidal aggregates (~ 105 nm) of fine particles (5-10 nm)	The band gap shift (quantum size effect), Capping agent (L-cysteine)	Extracellular		[129]
	Cubic and hexagonal PbS	Torulopsis	Spherical, 2-5 nm	Small bandgap	Intracellular		[130]
	Cubic PbS	Rhodosporidium diobovatum	Spherical, well-dispersed, 2-5 nm	Capping agent coating with protein-bound thiols	Intracellular		[131]
	Tetragonal PbS_2 (β-PbS_2)	Idiomarina sp. strain PR58-8	Spherical, 2-10 nm		Intracellular		[133]
	CdS, PbS	Bacillus megaterium	10-20 nm	pH value (yield), no H_2S production	Extracellular		[156]
Other metal sulfide	MnS (rambergite)	Shewanella oneidensis MR-1	Aggregates (50-200 nm) of fine particles	EPS	Epicellular, extracellular		[157]
	Monoclinic Ag_2S	Pseudomonas stutzeri AG259	Equilateral triangles and hexagons, up to 200 nm		Extracelllar, epicellular, intracellular(periplasm)		[134]

	Ag_2S (acanthite)	Mixed culture of Thiobadllus ferroxidans and Thiobacillus thiooxidans	Spherical, tens of nm		Epicellular		[135]
	Ag_2S	Candida albicans, Candida glabrata			Extracellular		[136]
	HgS (cinnabar), Cubic PbS (galena), cubic CdS (hawleyite)	Candida species (C. albicans, C. glabrata, C. krusei, C. Parapsilosis)	Bunch-like clusters (CdS)		Intracellular(HgS, CdS), epicelluar(PbS)		[158]

Acknowledgments

The authors would like to thank the MEM group of the BIAM for support. Emilie Gachon and Dan Chevrier are particularly acknowledged for proofreading. Yeseul Park's PhD thesis is funded by the CEA. In addition, research in Damien Faivre's group is supported by the CEA, the ANR and the Excellence Initiative of Aix-Marseille Université – A*Midex, a French "Investissements d'Avenir" program.

Conflict of interest

The authors declare no conflict of interest.

Keywords

Biologically-controlled biomineralization • biologically-induced biomineralization • biologically-influenced biomineralization • Biomineralization; biomolecules • capping agent • epicellular biomineralization • extracellular biomineralization • intracellular biomineralization • metal sulfide • metal sulfide nanoparticles • organic matrix

References

[1] P. Chandrangsu, C. Rensing, J. D. Helmann, *Nat. Rev. Microbiol* **2017**, *15*, 338–350.
[2] R. Jing, B. V. Kjellerup, *J. Environ. Sci.* **2018**, *66*, 146–154.
[3] G. Kuippers, C. Boothman, H. Bagshaw, M. Ward, R. Beard, N. Bryan, J. R. Lloyd, *Sci. Rep.* **2018**, *8*, 8753.
[4] K. Chojnacka, *Environ. Int.* **2010**, *36*, 299–307.
[5] K. Bosecker, *FEMS Microbiol. Rev.* **1997**, *20*, 591–604.
[6] J. Kirtzel, N. Ueberschaar, T. Deckert-Gaudig, K. Krause, V. Deckert, G. M. Gadd, E. Kothe, *Environ. Microbiol.* **2020**, *22*, 1535–1546.
[7] D. E. Rawlings, *Microb. Cell Fact.* **2005**, *4*, 13.
[8] C.-H. Lai, M.-Y. Lu, L.-J. Chen, *J. Mater. Chem.* **2012**, *22*, 19–30.
[9] Y. Li, N. Kitadai, R. Nakamura, *Life* **2018**, *8*, 46.
[10] M. Mansor, D. Berti, M. F. H. Jr, M. Murayama, J. Xu, *Am. Mineral.* **2019**, *104*, 703–717.
[11] G. W. Luther, D. T. Rickard, *J. Nanopart. Res.* **2005**, *7*, 389–407.
[12] D. J. Vaughan, C. L. Corkhill, *Elements* **2017**, *13*, 81–87.
[13] S. Chandrasekaran, L. Yao, L. Deng, C. Bowen, Y. Zhang, S. Chen, Z. Lin, F. Peng, P. Zhang, *Chem. Soc. Rev.* **2019**, *48*, 4178–4280.
[14] J. Wang, S. Lin, N. Tian, T. Ma, Y. Zhang, H. Huang, *Adv. Funct. Mater.* **2021**, *31*, 2008008.
[15] P. Kulkarni, S. K. Nataraj, R. G. Balakrishna, D. H. Nagaraju, M. V. Reddy, *J. Mater. Chem. A* **2017**, *5*, 22040–22094.
[16] X. Yang, H.-J. Liang, H.-Y. Yu, M.-Y. Wang, X.-X. Zhao, X.-T. Wang, X.-L. Wu, *J. Phys. Mater.* **2020**, *3*, 042004.
[17] J. R. Craig, D. J. Vaughan, in *Sulphide Deposits—Their Origin and Processing* (Eds.: P.M.J. Gray, G.J.

Bowyer, J.F. Castle, D.J. Vaughan, N.A. Warner), Springer Netherlands, Dordrecht, **1990**, pp. 1–16.
[18] D. J. Vaughan, in *Encyclopedia of Geology* (Eds.: R.C. Selley, L.R.M. Cocks, I.R. Plimer), Elsevier, Oxford, **2005**, pp. 574–586.
[19] J. R. Craig, S. D. Scott, in *Sulfide Mineralogy*, De Gruyter, **2018**, pp. 124–233.
[20] T. Kasama, M. Pósfai, R. K. K. Chong, A. P. Finlayson, P. R. Buseck, R. B. Frankel, R. E. Dunin-Borkowski, *Am. Mineral.* **2006**, *91*, 1216–1229.
[21] D. A. Bazylinski, R. B. Frankel, *Nat. Rev. Microbiol.* **2004**, *2*, 217–230.
[22] S. A. Kumar, M. K. Abyaneh, S. W. Gosavi, S. K. Kulkarni, R. Pasricha, A. Ahmad, M. I. Khan, *Biotechnol. Lett.* **2007**, *29*, 439–445.
[23] C. K. Carney, S. R. Harry, S. L. Sewell, D. W. Wright, in *Biomineralization I: Crystallization and Self-Organization Process* (Ed.: K. Naka), Springer Berlin Heidelberg, Berlin, Heidelberg, **2007**, pp. 155–185.
[24] H. Ehrlich, E. Bailey, M. Wysokowski, T. Jesionowski, *Biomimetics* **2021**, *6*, 46.
[25] D. V. Meier, P. Pjevac, W. Bach, S. Markert, T. Schweder, J. Jamieson, S. Petersen, R. Amann, A. Meyerdierks, *Environ. Microbiol.* **2019**, *21*, 682–701.
[26] C. A. Dehner, J. D. Awaya. P. Maurice, J. L. Dubois, J. *Rev. Microbiol.* **2010**, *76*, 2041–2048.
[27] H. R. Watling, *Minerals* **2015**, *5*, 1–60.
[28] O. Y. A. Costa, J. M. Raaijmakers, E. E. Kuramae, *Front. Microbiol.* **2018**, *9*, 1636.
[29] T. Rohwerder, T. Gehrke, K. Kinzler, W. Sand, *Appl. Microbiol. Biotechnol.* **2003**, *63*, 239–248.
[30] S. Bellenberg, B. Salas, S. Ganji, C. Jorquera-Román, M. L. Valenzuela, A. Buetti-Dinh, C. R. Unelius, M. Dopson, M. Vera, *Sci. Rep.* **2021**, *11*, 16275.
[31] Y. Jia, Q. Tan, H. Sun, Y. Zhang, H. Gao, R. Ruan, *Green Energy Environ.* **2019**, *4*, 29–37.
[32] T. O. Ferreira, X. L. Otero, P. Vidal-Torrado, F. Macías, *Geoderma* **2007**, *142*, 36–46.
[33] D. E. Canfield, J. Farquhar, in *Fundamentals of Geobiology*, John Wiley & Sons, Ltd, **2012**, pp. 49–64.
[34] A. E. Konopka, R. H. Miller, L. E. Sommers, in *Sulfur in Agriculture*, John Wiley & Sons, Ltd, **1986**, pp. 23–55.
[35] B. B. Jørgensen, A. J. Findlay, A. Pellerin, *Front. Microbiol.* **2019**, *10*, 849.
[36] D. A. Fike, A. S. Bradley, C. V. Rose, *Annu. Rev. Earth Planet. Sci.* **2015**, *43*, 593–622.
[37] A. Picard, A. Gartman, P. R. Girguis, *Front. Earth Sci.* **2016**, *4*, 68.
[38] D. Bhattacharyya, A. B. Jumawan, R. B. Grieves, *Sep. Sci. Technol.* **1979**, *14*, 441–452.
[39] E. Peltier, P. Ilipilla, D. Fowle, *Appl. Geochem.* **2011**, *26*, 1673–1680.
[40] M. Pósfai, R. E. Dunin-Borkowski, *Rev. Mineral. Geochem.* **2006**, *61*, 679–714.
[41] N. Duran, A. B. Seabra, *Curr. Biotechnol.* **2012**, *1*, 287–296.
[42] R. Javed, M. Zia, S. Naz, S. O. Aisida, N. ul Ain, Q. Ao, *J. Nanobiotechnol.* **2020**, *18*, 172.
[43] S. Campisi, M. Schiavoni, C. E. Chan-Thaw, A. Villa, *Catalysts* **2016**, *6*, 185.
[44] R. B. Frankel, in *Iron Biominerals* (Eds.: R.B. Frankel, R.P. Blakemore), Springer US, Boston, MA, **1991**, pp. 1–6.
[45] J.-F. Päßler, E. Jarochowska, M. Bestmann, A. Munnecke, *Front. Earth Sci.* **2018**, *6*, 16.
[46] S. Weiner, P. M. Dove, *Rev. Mineral. Geochem.* **2003**, 54, 1–29.
[47] A. W. Decho, Ecol. Eng. **2011**, *36*, 137–144.
[48] C. Dupraz, R. Reid, O. Braissant, A. Decho, R. Norman, P. Visscher, *Earth-Sci. Rev.* **2009**, *96*, 141–162.
[49] G. Long, P. Zhu, Y. Shen, M. Tong, *Environ. Sci. Technol.* **2009**, *43*, 2308–2314.
[50] J. Wang, Q. Li, M.-M. Li, T.-H. Chen, Y.-F. Zhou, Z.-B. Yue, *Bioresour. Technol.* **2014**, *163*, 374–376.
[51] Y. Salama, M. Chennaoui, A. Sylla, M. Mountadar, M. Rihani, O. Assobhei, *Desalin. Water Treat.* **2016**, *57*, 16220–16237.
[52] F. Yang, H. Li, S. Wang, F. Zhao, F. Fang, J. Guo, M. Long, Y. Shen, *Environ. Technol.* **2021**, *0*, 1–13.
[53] K. Cremin, B. A. Jones, J. Teahan, G. N. Meloni, D. Perry, C. Zerfass, M. Asally, O. S. Soyer, P. R. Unwin, *Anal. Chem.* **2020**, *92*, 16024–16032.
[54] K. Konhauser, R. Riding, in *Fundamentals of Geobiology*, John Wiley & Sons, Ltd, **2012**, pp. 105–130.
[55] R. B. Frankel, D. A. Bazylinski, *Rev. Mineral. Geochem.* **2003**, *54*, 95–114.
[56] A. Rao, H. Cölfen, *Biophys. Rev.* **2016**, *8*, 309–329.
[57] S. Görgen, K. Benzerara, F. Skouri-Panet, M. Gugger, F. Chauvat, C. Cassier-Chauvat, *Discov. Mater.* **2021**, *1*, 2.
[58] H. A. Lowenstam, *Science* **1981**, *211*, 1126–1131.
[59] H. A. Lowenstam, S. Weiner, in *Biomineralization and Biological Metal Accumulation* (Eds.: P. Westbroek, E. W. de Jong), Springer Netherlands, Dordrecht, **1989**, pp. 191–203.
[60] A. Veis, in *Biomineralization* (Eds.: A. Sigel, H. Sigel, R.K.O. Sigel), John Wiley & Sons, Ltd, **2008**, pp.

1–35.
[61] A. Pandey, A. K. Patel, K. Balani, in *Biosurfaces: A Materials Science and Engineering Perspective* (Eds.: K. Balani, V. Verma, A. Agarwal, R. Narayan), John Wiley & Sons, **2015**, pp. 65–105.
[62] G. Billon, B. Ouddane, J. Laureyns, A. Boughriet, *Phys. Chem. Chem. Phys.* **2001**, *3*, 3586–3592.
[63] A. P. Abbott, A. Z. M. Al-Bassam, A. Goddard, R. C. Harris, G. R. T. Jenkin, F. J. Nisbet, M. Wieland, *Green Chem.* **2017**, *19*, 2225–2233.
[64] D. J. Vaughan, A. R. Lennie, *Sci. Prog. (1933-)* **1991**, *75*, 371–388.
[65] Y. Yuan, L. Wang, L. Gao, *Front. Chem.* **2020**, *8*, 818.
[66] M. Posfai, P. R. Buseck, D. A. Bazylinski, R. B. Frankel, *Am. Mineral.* **1998**, *83*, 1469–1481.
[67] M. Pósfai, C. Lefèvre, D. Trubitsyn, D. A. Bazylinski, R. Frankel, *Front. Microbiol.* **2013**, *4*, 344.
[68] A. Duverger, J. S. Berg, V. Busigny, F. Guyot, S. Bernard, J. Miot, *Front. Earth Sci.* **2020**, *8*, 457.
[69] J. S. Berg, A. Duverger, L. Cordier, C. Laberty-Robert, F. Guyot, J. Miot, *Sci. Rep.* **2020**, *10*, 8264.
[70] A. Picard, A. Gartman, D. R. Clarke, P. R. Girguis, *Geochim. Cosmochim. Acta* **2018**, *220*, 367–384.
[71] R. Donald, G. Southam, *Geochim. Cosmochim. Acta* **1999**, *63*, 2019–2023.
[72] J. H. P. Watson, B. A. Cressey, A. P. Roberts, D. C. Ellwood, J. M. Charnock, A. K. Soper, *J. Magn. Magn. Mater.* **2000**, *214*, 13–30.
[73] H. E. Jones, P. A. Trudinger, L. A. Chambers, N. A. Pyliotis, *Z. Allg. Mikrobiol.* **1976**, *16*, 425–435.
[74] B. H. Lower, D. A. Bazylinski, *Microb. Physiol.* **2013**, *23*, 63–80.
[75] C. T. Lefèvre, D. A. Bazylinski, *Microbiol. Mol. Biol. Rev.* **2013**, *77*, 497–526.
[76] W. Lin, Y. Pan, *Environ. Microbiol. Rep.* **2015**, *7*, 237–242.
[77] C. T. Lefèvre, D. Trubitsyn, F. Abreu, S. Kolinko, C. Jogler, L. G. P. de Almeida, A. T. R. de Vasconcelos, M. Kube, R. Reinhardt, U. Lins, D. Pignol, D. Schüler, D. A. Bazylinski, N. Ginet, *Environ. Microbiol.* **2013**, *15*, 2712–2735.
[78] C. T. Lefèvre, N. Menguy, F. Abreu, U. Lins, M. Pósfai, T. Prozorov, D. Pignol, R. B. Frankel, D. A. Bazylinski, *Science* **2011**, *334*, 1720–1723.
[79] R. Wenter, G. Wanner, D. Schüler, J. Overmann, *Environ. Microbiol.* **2009**, *11*, 1493–1505.
[80] J. J. Jacob, K. Suthindhiran, *Mater. Sci. Eng. C* **2016**, *68*, 919–928.
[81] D. A. Bazylinski, A. J. Garratt-Reed, R. B. Frankel, *Microsc. Res. Tech.* **1994**, *27*, 389–401.
[82] B. R. Heywood, S. Manna, R. B. Frankelb, *MRS Proc.* **1990**, *218*, 93.
[83] S. Mann, N. H. C. Sparks, R. B. Frankel, D. A. Bazylinski, H. W. Jannasch, *Nature* **1990**, *343*, 258–261.
[84] M. Farina, D. M. S. Esquivel, H. G. P. L. de Barros, *Nature* **1990**, *343*, 256–258.
[85] M. Pósfai, P. R. Buseck, D. A. Bazylinski, R. B. Frankel, *Science* **1998**, *280*, 880–883.
[86] D. A. Spears, M. R. Martinez Tarazona, S. Lee, *Fuel* **1994**, *73*, 1051–1055.
[87] B. P. von der Heyden, A. N. Roychoudhury, *Curr. Pollut. Rep.* **2015**, *1*, 265–279.
[88] M. F. Kirk, E. E. Roden, L. J. Crossey, A. J. Brealey, M. N. Spilde, *Geochim. Cosmochim. Acta* **2010**, *74*, 2538–2555.
[89] M. Wolthers, I. B. Butler, D. Rickard, *Chem. Geol.* **2007**, *236*, 217–227.
[90] D. Fortin, G. Southam, T. J. Beveridge, *FEMS Microbiol. Ecol.* **1994**, *14*, 121–132.
[91] M. Mansor, C. Winkler, M. F. Hochella, J. Xu, *Front. Earth Sci.* **2019**, *7*, 151.
[92] J. P. Gramp, K. Sasaki, J. M. Bigham, O. V. Karnachuk, O. H. Tuovinen, *Geomicrobiol. J.* **2006**, *23*, 613–619.
[93] M. Cowper, D. Rickard, *Chem. Geol.* **1989**, *78*, 325–341.
[94] D. A. Bazylinski, A. J. Garratt-Reed, A. Abedi, R. B. Frankel, *Arch. Microbiol.* **1993**, *160*, 35–42.
[95] J. Sitte, K. Pollok, F. Langenhorst, K. Küsel, *Geomicrobiol. J.* **2013**, *30*, 36–47.
[96] J. P. Gramp, J. M. Bigham, K. Sasaki, O. H. Tuovinen, *Geomicrobiol. J.* **2007**, *24*, 609–614.
[97] Y. Liu, A. Serrano, J. Vaughan, G. Southam, L. Zhao, D. Villa-Gomez, *Hydrometallurgy* **2019**, *189*, 105142.
[98] M. Bhagat, J. E. Burgess, A. P. M. Antunes, C. G. Whiteley, J. R. Duncan, *Miner. Eng.* **2004**, *17*, 925–932.
[99] J. W. Morse, G. W. Luther, *Geochim. Cosmochim. Acta* **1999**, *63*, 3373–3378.
[100] A. E. Lewis, *Hydrometallurgy* **2010**, *104*, 222–234.
[101] M. R. Hosseini, M. Schaffie, M. Pazouki, E. Darezereshki, M. Ranjbar, *Mater. Sci. Semicond. Process.* **2012**, *15*, 222–225.
[102] R. L. Kimber, H. Bagshaw, K. Smith, D. M. Buchanan, V. S. Coker, J. S. Cavet, J. R. Lloyd, *Appl. Environ. Microbiol.* **2020**, *86*, e00967-20.
[103] S. Yoon, C. Yáñez, M. A. Bruns, N. Martínez-Villegas, C. E. Martínez, *Geochim. Cosmochim. Acta* **2012**, *84*, 165–176.
[104] J. W. Moreau, P. K. Weber, M. C. Martin, B. Gilbert, I. D. Hutcheon, J. F. Banfield, *Science* **2007**, *316*,

1600.
[105] J. W. Moreau, R. I. Webb, J. F. Banfield, *Am. Mineral.* **2004**, *89*, 950–960.
[106] J. A. Raven, A. H. Knoll, *Geomicrobiol. J.* **2010**, *27*, 572–584.
[107] L. Karygianni, Z. Ren, H. Koo, T. Thurnheer, *Trends Microbiol.* **2020**, *28*, 668–681.
[108] J. Liu, N. Soler, A. Gorlas, V. Cvirkaite-Krupovic, M. Krupovic, P. Forterre, *microLife* **2021**, *2*, uqab007.
[109] C. Malarkodi, G. Annadurai, *Appl. Nanosci.* **2013**, *3*, 389–395.
[110] P. Uddandarao, R. M. B, *Mater. Sci. Eng. B* **2016**, *207*, 26–32.
[111] L. Rodriguez-Freire, R. Sierra-Alvarez, R. Root, J. Chorover, J. A. Field, *Water Res.* **2014**, *66*, 242–253.
[112] Newman D K, Beveridge T J, Morel F, *Appl. Environ. Microbiol.* **1997**, *63*, 2022–2028.
[113] J.-H. Lee, M.-G. Kim, B. Yoo, N. V. Myung, J. Maeng, T. Lee, A. C. Dohnalkova, J. K. Fredrickson, M. J. Sadowsky, H.-G. Hur, *PNAS* **2007**, *104*, 20410–20415.
[114] S. Jiang, J.-H. Lee, M.-G. Kim, N. V. Myung, J. K. Fredrickson, M. J. Sadowsky, H.-G. Hur, *Appl. Environ. Microbiol.* **2009**, *75*, 6896–6899.
[115] J. Tourney, B. T. Ngwenya, *Chem. Geol.* **2009**, *262*, 138–146.
[116] H. Ehrlich, M. Motylenko, P. V. Sundareshwar, A. Ereskovsky, I. Zgłobicka, T. Noga, T. Płociński, M. V. Tsurkan, E. Wyroba, S. Suski, H. Bilski, M. Wysokowski, H. Stöcker, A. Makarova, D. Vyalikh, J. Walter, S. L. Molodtsov, V. V. Bazhenov, I. Petrenko, E. Langer, A. Richter, E. Niederschlag, M. Pisarek, A. Springer, M. Gelinsky, D. Rafaja, A. Witkowski, D. C. Meyer, T. Jesionowski, K. J. Kurzydłowski, *Adv. Funct. Mater.* **2016**, *26*, 2503–2510.
[117] V. M. Dekov, L. Bindi, G. Burgaud, S. Petersen, D. Asael, V. Rédou, Y. Fouquet, B. Pracejus, *Mar. Geol.* **2013**, *342*, 28–38.
[118] N. Ma, Z. Sha, C. Sun, *Environ. Microbiol.* **2021**, *23*, 934–948.
[119] R. Dunleavy, L. Lu, C. J. Kiely, S. McIntosh, B. W. Berger, *PNAS* **2016**, *113*, 5275–5280.
[120] N. Ma, R. Cai, C. Sun, *J. Hazard. Mater.* **2021**, *417*, 126102.
[121] A. Ahmad, P. Mukherjee, D. Mandal, S. Senapati, M. I. Khan, R. Kumar, M. Sastry, *J. Am. Chem. Soc.* **2002**, *124*, 12108–12109.
[122] C. T. Dameron, R. N. Reese, R. K. Mehra, A. R. Kortan, P. J. Carroll, M. L. Steigerwald, L. E. Brus, D. R. Winge, *Nature* **1989**, *338*, 596–597.
[123] S. Balzano, A. Sardo, M. Blasio, T. B. Chahine, F. Dell'Anno, C. Sansone, C. Brunet, *Front. Microbiol.* **2020**, *11*, 517.
[124] W. E. Rauser, *Annu. Rev. Biochem.* **1990**, *59*, 61–86.
[125] J. Huang, Y. Zhang, J.-S. Peng, C. Zhong, H.-Y. Yi, D. W. Ow, J.-M. Gong, *Plant Physiol.* **2012**, *158*, 1779–1788.
[126] W. Bae, X. Chen, *Mol. Cell. Proteomics* **2004**, *3*, 596–607.
[127] N. Krumov, S. Oder, I. Perner-Nochta, A. Angelov, C. Posten, *J. Biotechnol.* **2007**, *132*, 481–486.
[128] C. T. Dameron, D. R. Winge, *Inorg. Chem.* **1990**, *29*, 1343–1348.
[129] S. Wei, C. Guo, L. Wang, J. Xu, H. Dong, *Sci. Rep.* **2021**, *11*, 1216.
[130] M. Kowshik, W. Vogel, J. Urban, S. K. Kulkarni, K. M. Paknikar, *Adv. Mater.* **2002**, *14*, 815–818.
[131] S. Seshadri, K. Saranya, M. Kowshik, *Biotechnol. Prog.* **2011**, *27*, 1464–1469.
[132] M. Cuéllar-Cruz, G. Gutiérrez-Sánchez, E. López-Romero, E. Ruiz-Baca, J. C. Villagómez-Castro, L. Rodríguez-Sifuentes, *Cent. Eur. J. Biol.* **2013**, *8*, 337–345.
[133] P. Srivastava, M. Kowshik, *Appl. Environ. Microbiol.* **2017**, *83*, e03091-16.
[134] T. Klaus, R. Joerger, E. Olsson, C.-G. Granqvist, *PNAS* **1999**, *96*, 13611–13614.
[135] F. D. Pooley, *Nature* **1982**, *296*, 642–643.
[136] A. Moreno, D. Lucio-Hernández, M. Cuéllar-Cruz, *Rev. Iberoam. Micol.* **2019**, *36*, 120–128.
[137] D. Bazylinski, R. Frankel, *Rev. Mineral. Geochem.* **2003**, *54*, 217–247.
[138] A. Gorlas, P. Jacquemot, J.-M. Guigner, S. Gill, P. Forterre, F. Guyot, *PLOS One* **2018**, *13*, e0201549.
[139] X. Deng, N. Dohmae, A. H. Kaksonen, A. Okamoto, *Angew. Chem., Int. Ed.* **2020**, *59*, 5995–5999.
[140] C. Zhou, R. Vannela, K. F. Hayes, B. E. Rittmann, *J. Hazard. Mater.* **2014**, *272*, 28–35.
[141] F. Abreu, J. L. Martins, T. S. Silveira, C. N. Keim, H. G. P. L. de Barros, F. J. G. Filho, U. 2007 Lins, *Int. J. Syst. Evol. Microbiol.* **2007**, *57*, 1318–1322.
[142] Y.-R. Chen, R. Zhang, H.-J. Du, H.-M. Pan, W.-Y. Zhang, K. Zhou, J.-H. Li, T. Xiao, L.-F. Wu, *Environ. Microbiol.* **2015**, *17*, 637–647.
[143] D. A. Bazylinski, R. B. Frankel, A. J. Garratt-Reed, S. Mann, in *Iron Biominerals* (Eds.: R.B. Frankel, R.P. Blakemore), Springer US, Boston, MA, **1991**, pp. 239–255.
[144] Y. Liu, A. Serrano, V. Wyman, E. Marcellin, G. Southam, J. Vaughan, D. Villa-Gomez, *J. Hazard. Mater.*

2021, *402*, 123506.
[145] C. White, G. M. Gadd, *FEMS Microbiol. Lett.* **2000**, *183*, 313–318.
[146] H.-J. Bai, Z.-M. Zhang, J. Gong, *Biotechnol. Lett.* **2006**, *28*, 1135–1139.
[147] M. Labrenz, G. K. Druschel, T. Thomsen-Ebert, B. Gilbert, S. A. Welch, K. M. Kemner, G. A. Logan, R. E. Summons, G. D. Stasio, P. L. Bond, B. Lai, S. D. Kelly, J. F. Banfield, *Science* **2000**, *290*, 1744–1747.
[148] J.-W. Moon, I. N. Ivanov, P. C. Joshi, B. L. Armstrong, W. Wang, H. Jung, A. J. Rondinone, G. E. Jellison, H. M. Meyer, G. G. Jang, R. A. Meisner, C. E. Duty, T. J. Phelps, *Acta Biomater.* **2014**, *10*, 4474–4483.
[149] J. G. Sandana Mala, C. Rose, *J. Biotechnol.* **2014**, *170*, 73–78.
[150] R. N. Ledbetter, S. A. Connon, A. L. Neal, A. Dohnalkova, T. S. Magnuson, *Appl. Environ. Microbiol.* **2007**, *73*, 5928–5936.
[151] N. Ma, C. Sun, *Environ. Microbiol. Rep.* **2021**, *13*, 325–336.
[152] D. P. Cunningham, L. L. Lundie, *Appl. Environ. Microbiol.* **1993**, *59*, 7–14.
[153] R. Y. Sweeney, C. Mao, X. Gao, J. L. Burt, A. M. Belcher, G. Georgiou, B. L. Iverson, *Chem. Biol.* **2004**, *11*, 1553–1559.
[154] H. J. Bai, Z. M. Zhang, Y. Guo, G. E. Yang, *Colloids Surf., B* **2009**, *70*, 142–146.
[155] L. C. Staicu, P. J. Wojtowicz, M. Pósfai, P. Pekker, A. Gorecki, F. L. Jordan, L. L. Barton, *FEMS Microbiol. Ecol.* **2020**, *96*, fiaa151.
[156] A. Prakash, S. Sharma, N. Ahmad, A. Ghosh, P. Sinha, *Int. Res. J. Biotechnol.* **2011**, *1*, 2141–5153071.
[157] J.-H. Lee, D. W. Kennedy, A. Dohnalkova, D. A. Moore, P. Nachimuthu, S. B. Reed, J. K. Fredrickson, *Environ. Microbiol.* **2011**, *13*, 3275–3288.
[158] M. Cuéllar-Cruz, D. Lucio-Hernández, I. Martínez-Ángeles, N. Demitri, M. Polentarutti, M. J. Rosales-Hoz, A. Moreno, *Microb. Biotechnol.* **2017**, *10*, 405–424.

Biographies

Yeseul Park

Yeseul Park obtained her BSc in chemistry and nanoscience in 2013 from the Ewha Womans University (SIP). She completed a material science MSc program organized by the Technical university of Munich, the University of Augsburg and the University of Munich. She worked at BASF and at Max Planck Institute for Polymer research as a research intern and later at LG electronics. Currently, she is pursuing her Ph.D. at Aix-Marseille University in France, working at CEA Cadarache under the supervision of Dr. Damien Faivre with focus on biomineralization of magnetic materials and metal sulfides.

Dr. Damien Faivre

I am broadly interested by the interactions between life and inanimate. I looked for traces of Life on rocks during my PhD (Institute of Earth Physics, Paris, France; and Caltech, Pasdena, USA). I tried forming nanoparticles with controlled properties using biomacromolecules during my post doc (Max Planck Institute of Marine Microbiology, Bremen, Germany). My group (Max Planck Institute of Colloids and Interfaces, Potsdam, Germany) studied calcite biomineralization, the effect of nanoparticles on eukaryotic cells, microswimmers or how magnetic nanoparticles can be used in a medical context. I finally joined the Bioscience and Biotechnology Institute of Aix Marseille in 2018 (CEA Cadarache, France) where I continue this diverse research.

A Table of Contents

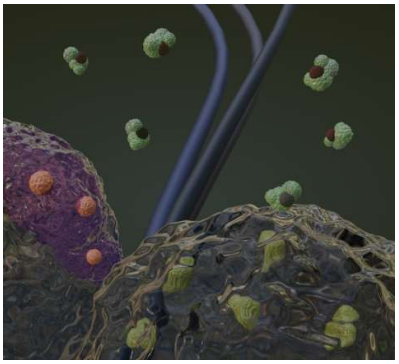

In this review paper, types of general interactions among microorganisms with metal species are first discussed, which is followed by general classification of microbial biomineralization. In this context, distinctive features and mechanisms found in biomineralization of metal sulfides are introduced with several examples by the atomic order. Some environmental factors are presented, together with biogenic molecules that are used to regulate biomineral properties. Finally, common factors for unique features in each biomineral are summarized with authors' general remarks on biological control in biomineralization.